Micromechanical Modeling of Anisotropic Creep and Damage Development in Metal Matrix Composites with Tension-Compression Asymmetry

Alexander Zolochevsky

ALEXANDER ZOLOCHEVSKY

Micromechanical Modeling of Anisotropic Creep and Damage Development in Metal Matrix Composites with Tension-Compression Asymmetry

Research Center «Polytech», Kharkiv, Ukraine
e-mail: zolochevsky55@ukr.net

ABSTRACT. The report involves experimental data, constitutive modeling, analytical, analytical-numerical and numerical methods, as well as, computational investigations towards an understanding the damage growth in metal matrix composites with periodically distributed fibers at high temperatures and creep conditions within the framework of micromechanical approach and representative volume element. Development of damage in metal matrix composites has been analyzed for such composite constituents as matrix, reinforcement, interfaces and coating. The constitutive laws of elastoplastic deformation and anisotropic creep at high temperatures, as well as, the kinetic equations of damage growth have been considered. Tension-compression asymmetry of composite constituents and initial anisotropy of matrix materials were taken into account. Implementation of the integrated constitutive model into ABAQUS, ANSYS and in-house developed software has been considered in a form of the computer-based structural modeling tools to assess the stress redistribution over time throughout the metal matrix composite, as well as, for damage analysis and for lifetime prediction studies. The outcome of this analysis is related to the practical recommendations on how damage growth in metal matrix composites may be controlled in order to reduce materials degradation over time, and extend lifetime of metal matrix composites in high temperature applications.

KEY WORDS: Micromechanics, metal matrix composite, representative volume element, creep, damage, constitutive modeling, lifetime prediction

How to cite this research: Zolochevsky Alexander. Micromechanical Modeling of Anisotropic Creep and Damage Development in Metal Matrix Composites with Tension-Compression Asymmetry. Technical Report, Research Center «Polytech», Kharkiv, Ukraine, 2022, 28p.

1. Introduction

At present, Metal Matrix Composites (MMCs) have been intensively developed due to the number of important applications. All MMCs have a metal (or a metallic alloy) as the matrix. There are four kinds of MMCs [1]:
1). Particle-reinforced MMCs;
2). Short fiber- (or whisker-reinforced) MMCs;
3). Continuous fiber- (or sheet-reinforced) MMCs;
4). Laminated (or layered) MMCs.

Common matrix metallic materials are Aluminum and Aluminum Alloys, Titanium Alloys, Magnesium and its Alloys, Cobalt, Copper, Silver, Nickel, Iron, Niobium and Intermetallics. The reinforcement can be metallic or ceramic. Recently, novel MMCs reinforced by graphene were developed [2], and it was found that MMCs reinforced by those particles give competitive economical and isotropic characteristics at high temperatures.

In this report, special attention will be given to short fiber- and continuous fiber unidirectional MMCs. In particular, continuously reinforced MMCs, such as *silicon carbide fiber reinforced titanium matrix composites*, are one of the candidate materials in rotating components of gas turbines for aerospace applications at temperatures up to 550°C [3]. These composites are stronger, more temperature resistant and have a lower weight to stiffness ratio than conventional metal alloys [4]. New fabrication methods for MMCs including physical vapor deposition and additive manufacturing were developed for aerospace applications [5].

The functionality and reliability of MMCs at high temperatures are strongly related to the damage growth and stresses redistribution over time in the structures. A methodology for durability analysis of MMCs is needed that includes experimental investigations, as well as, constitutive and numerical modeling.

The thermomechanical properties of MMCs are determined by a combination of the properties of the microstructural phases and the internal architecture formed by them. This architecture must be described using 3D techniques taking into account that the phases are distributed nonuniformly in MMCs, have complex morphologies, form interconnected structures and present contiguity between those structures [6]. Furthermore, all these

morphological aspects may change under thermomechanical cyclic loading. Development of synchrotron tomography using high energy synchrotron radiation gives the possibility to reveal the 3D structure of heterogeneous materials with sub-micrometer spatial resolution, as well as, the length scale, where the basic mechanisms of inelastic deformation and damage take place, and determine the macroscopic behavior of MMCs [6]. In this way, the 3D microstructure of a whisker reinforced titanium alloy has been studied, and practical recommendations related to the damage development have been formulated [6]. Also, the growth of creep damage in MMCs has been investigated using X-ray tomography, and the necessary experimental data have been provided for validating numerical simulations of creep damage evolution, e.g., by Monte Carlo methods or finite element simulations [7]. Additionally, the evolution of fatigue damage in a 35vol% SiC fiber/titanium alloy composite has been studied using X-ray computed tomography [7]. Different damage mechanisms found earlier in carbon fiber reinforced epoxy laminates [8] were investigated from the tomographies in MMC deformed during tensile testing [7], such as, matrix cracking, interply delamination, fiber-matrix debonding and fiber cracking.

Thus, synchrotron tomography using high energy synchrotron radiation provides a thorough knowledge of creep behaviors and damage mechanisms of fiber reinforced composite materials at elevated temperature which are required for their engineering applications. However, such experiments are costly and time consuming, and, therefore, the development of simulation methods for predicting creep and damage growth in MMCs is also necessary.

In general, there are two types of studies in nonlinear mechanics of composites commonly referred to as macromechanical and micromechanical. *Macromechanical studies* of composite materials are done at the macrostructural level using homogenized nonlinear properties of composites including nonlinear elasticity, elastoplastic deformation, creep and damage evolution related to the initial anisotropy and tension-compression material asymmetry [9-23]. In contrary, *micromechanical studies* of composite materials are based on the reinforcement/matrix interactions and properties of composite constituents (matrix, reinforcement, interfaces and coating) at the microstructural level, as well as, on the various homogenization techniques [24-27].

As a rule, micromechanical modeling of MMCs with *periodically* distributed fibers assumes the consideration of a repeating unit cell that serves as *representative volume element* (RVE) of a periodic composite material. This means that the RVE must be statistically equivalent to a real microstructure of composite under study. Most of the creep models in micromechanics of MMCs were used under assumption of the creep behavior of the metal matrix and linear elastic deformation of the fiber. Also, there are several methods in micromechanical modeling of periodic MMCs at high temperatures and creep conditions, such as, **analytical, analytical-numerical and numerical ones**. *There are no rigorous boundaries between these methods.*

Most of the *analytical methods* in creep micromechanics of MMCs are based on the two different approaches [28, 29]. The first one includes *the Eshelby* (mean stress or mean field) theory, which treats the strengthening of composites reinforced with elastic ellipsoidal inclusions. It is assumed that the inelastic strain in the matrix is uniform along the loading axis. The second one includes *the shear-lag* theories, in which strengthening was attributed to the load transfer through shear stresses from the matrix to the fiber at the interface along the loading axis.

A new analytical shear-lag based model for prediction of the steady state creep deformations of short fiber composites subjected to an applied axial load has been developed by Mondali et al. [30]. A perfect fiber/matrix interface is assumed, and the steady state creep behavior of the matrix is described by an exponential law. In the following, this analytical model was modified using Hermite polynomials, hyperbolic trigonometric functions and power series [31]. A novel analytical method has been discussed by Monfared [32] for predicting steady state creep of short fiber composites using shear-lag theory, imaginary fiber technique and polynomial displacement functions.

The objective of the paper by Li et al. [33] is to study the creep behavior and stress relaxation in the unidirectional fiber reinforced MMCs under biaxial loading. An analytical solution has been obtained using the Eshelby theory. Diffusion along the fiber/matrix interface and related creep are considered while the interface slip and the creep deformation of the matrix are not taken into account [33]. Based on the Eshelby theory, analytical solution for interfacial diffusion-induced creep of particulate MMCs under triaxial loading has been obtained by Sun et al. [34]. Also, analytical investigation of transverse creep in unidirectional fiber reinforced MMCs caused by diffusional relaxation and interface slip has been presented by Xu and Guo [35] using the Eshelby theory. In the following, such model was applied under general transverse loading conditions [36].

The difference between the Eshelby theory and the shear-lag model has been discussed by Fernandez and Gonzalez-Doncel [37] for the creep predictions in particle-reinforced MMCs. Eshelby model provides more rigorous predictions in composites with particles of low aspect ratio or when particles shape is close to an ellipsoid. On the other hand, shear-lag theory is expected to give good predictions in composites with elongated or large aspect ratio particles. Furthermore, it is much easier to use the shear-lag theory than Eshelby model in the analytical stress analysis.

A number of combined *analytical-numerical methods* were developed in micromechanics of inelastic composites [24-27]. **The computation time of such approach is reduced by at least an order relative to the pure numerical analysis.** A characteristic feature of such approach is the simultaneous use of various linearization techniques and homogenization theories, such as, self-consistent (Hill's) scheme, Mori-Tanaka theory, generalized self-consistent scheme, generalized method of cells, transformation field analysis, the asymptotic homogenization method, etc. Initially, the homogenization theories must be used in order to address the periodic boundary value problem for RVE of a periodic composite material. However, such approach has a number of limitations for practical use in the nonlinear analysis. The analytical-numerical methods were compared in the context of elastoplastic deformation of composites [38]. It is established that the transformation field analysis and the Mori-Tanaka method are preferred to the self-consistent estimate. An incremental secant mean-field homogenization procedure was developed for nonmonotonic loading for composites made of elastoplastic constituents [39]. The transformation field analysis was used to study the elastoviscoplasticity coupled with damage of a long fiber unidirectional metal matrix composite [40]. The generalized method of cells was applied to analyze the linear viscoelasticity of unidirectional composite [41]. The Mori-Tanaka scheme combined with the transformation field analysis was used to study the elastoviscoplasticity of composites [42]. A three-phase Mori-Tanaka method and transformation field analysis approach are developed within a unified framework that allows simulation of both ductile and discrete damages in different phases (fiber, matrix and interface) of composite materials [43]. In this way, the rate-dependent viscoelastic and viscoplastic response of the matrix phase was taken into account. The asymptotic homogenization method was used to investigate the 3D mechanical behavior of isotropic viscoelastic matrix reinforced by square (or hexagonal) arrangements of elastic transversely isotropic long (or short) fibers [44]. The finite volume based asymptotic homogenization was applied to viscoelastic unidirectional composites [45]. The matrix microcracking, interface debonding and interphase discrete damage at the fiber ends related to the elastoviscoplasticity of a short fiber reinforced composite were studied by Chen et al. [46] using the modified Mori-Tanaka method the transformation field analysis. The variational incremental mean-field homogenization model [47] was developed to analyze the elastoviscoplasticity of a periodic composite material. Predicting the viscoelastic behavior of unidirectional fiber reinforced composites based on the generalized self-consistent method was compared by Hine and Gusev [48] against available experimental data. A nonuniform transformation field analysis was done in [49] for composites with different elastoplastic characteristics under tension and compression, but without consideration of creep.

Note that *viscous material behavior means the sensitivity of the stress-strain response of a material to the rate of straining*. In general, the viscous response assumes that strain includes the viscous part (some function of time), as well as, elastic (reversible) and plastic (permanent) parts. Basically, **the elastoviscoplasticity of a material is similar to the high temperature creep behavior, however, in general, the long term creep deformation cannot be predicted satisfactorily by a model based on the elastoviscoplasticity.**

The Mori-Tanaka scheme was used by Chun and Daniel [50] to study transverse creep deformation in a unidirectional MMC. The high temperature deformation of short fiber reinforced MMCs including plasticity and creep was studied by Tsukamoto [51] using the Mori-Tanaka method. Creep of matrix and diffusional mass transfer at the interface are taken into account. The generalized method of cells was applied to analyze the creep deformation of a unidirectional composite subjected to longitudinal and/or transversal loading [52]. The asymptotic homogenization method was used by Wu and Ohno [53] to study the effect of fiber arrays on the anisotropy of creep in a unidirectional MMC. In the following, the theory of asymptotic homogenization of periodic media and Continuum Damage Mechanics were applied to analysis of nonlinear elastic deformation [54-56] and high temperature creep [57] of fiber reinforced composites subjected to a wide range of external loads taking into account matrix cracking, interface debonding, and fiber fracture and pull-out. Also, the generalized method of cells and Continuum Damage Mechanics were used by Khafagy et al. [58] to study the creep behavior of fiber reinforced composites. Additionally, the Mori-Tanaka method and Continuum Damage Mechanics coupled with the commercial finite element analysis software ANSYS were applied to analysis of elastoviscoplasticity of short fiber reinforced composites [59].

On the contrary, the use of pure *numerical methods* regarding the micromechanical modeling of nonlinear creep and damage in MMCs, in particular, the finite element method (FEM) together with linearization techniques has a number of advantages in comparison with the analytical-numerical methods because there are no restrictions on the geometry, material properties or number of phases in modeling. A comparison between FE approach and Mori-Tanaka theory was given for unidirectional fiber reinforced linear viscoelastic composites under transverse loading conditions [60, 61]. Nonlinear creep of composite constituents (matrix, fiber and interface) was not included in analysis [60, 61]. A FE technique has been formulated to study the elastoviscoplasticity of a SiC-Ti composite at the high temperature taking into account interface cracking [62]. It was established numerically that initial debonding is strongly influenced by thermal residual stresses. No long term creep was included in analysis. The FEM was used by Feyel and Chaboche [63] for modeling the elastoviscoplastic behaviour of long fibre SiC/titanium alloy composite. The two examples of simulation, such as, a beam subjected to bending and a reinforced compressor

disc subjected to centrifugal loading, have been considered [63]. The influence of the fiber/matrix interface strength on the macroscopic behavior and damage of composite has been discussed. The redistribution of stresses due to long term creep is not considered in these two examples. Nonlocal plasticity effects on the tensile properties of MMCs are analyzed by Niordson and Tvergaard [64]. The FE technique coupled with advanced contact algorithms [65, 66] gives the possibility to incorporate modeling the matrix–reinforcement assembly process, material temperature dependency as well as damage to study the elastoplastic deformation of SiC/Ti-15-3 unidirectional composite laminates. Again, the effect of creep was not considered in [65, 66]. The 3D FE micromechanical model was developed by Aghdam and Falahatgar [67] to study effects of thermal residual stress, fiber coating and interface bonding on the transverse behavior of a unidirectional long fiber SiC/ titanium alloy Ti–6Al–4V composite. The presented model takes into the consideration three phases, i.e. the fiber, coating and matrix, as well as, two distinct interfaces, one between the fiber and coating and the other between coating and matrix. The applicability of such model was to investigate effects of various bonding levels of the interfaces on the initiation of damage during transverse loading of MMC. Two different failure criteria, which are combinations of normal and shear stresses across the interfaces, were used to predict the failure of these interfaces. In the following, this micromechanical model for the SiC/ Ti–6Al–4V composite was employed by Aghdam et al. [68] and by Mahmoodi et al. [69] to study elastoplastic deformation and failure modes during biaxial tension/compression loading and under off-axis loading, respectively. The creep deformation was not considered here. The FE-based simulations performed in [70] show that the **consideration of the nonlinearity and the tension/compression-asymmetry seems to have the highest impact** on the elastoplasticity of unidirectional fiber reinforced composite.

Numerical modeling of the high-temperature longitudinal time dependent behavior of continuously reinforced titanium matrix composites (SiC/Ti-6242) has been done by Figiel and Günther [4]. In this way, the two viscoplastic matrix models have been used, such as, two-layer viscoplasticity model and the model of Chaboche, together with the FEM-based code ABAQUS and ANSYS, respectively. There is a good agreement between the simulated and experimental creep curves for SiC/Ti-6242 composite in its axial direction. A modeling approach associating a micromechanical analysis and a filament damage accumulation was developed to describe the creep behavior of continuous fiber reinforced titanium matrix composite in the longitudinal direction [71]. First, a numerical approach based on the cylindrical cell model and FEM provides an estimation of the average axial stress in the reinforcement during creep. Second, the critical value of this average stress which is necessary to predict the creep life of the composite is determined with the help of a filament damage accumulation model [71]. Modeling of the elastoplastic deformation and creep of continuously reinforced SiC/Ti-6242 composite has been performed by Martin and Carrére [72] using the RVE. Axial and transverse loadings have been analyzed with the help of a bidimensional plane strain FE analysis. The interfacial properties have been modeled with extreme conditions (perfectly bonded or completely debonded interface) or with the use of a stress debond criterion. The best choice remains to use a cohesive zone model [72]. Redistribution of stresses influenced by creep was studied by Ahmadi and Ataee in unidirectional fiber reinforced composite using the Norton power law and the FEM. An anisotropic creep behavior of unidirectional fiber reinforced composite was analyzed by Fliegener and Hohe [73] by employing the Kelvin-Voigt viscoelastic model and commercial FE software. Numerical modeling on creep responses of aligned short fiber reinforced composites was given by Wang and Smith [75] through the viscoelastic model with a Prony series expansion and ABAQUS software. Numerical simulation of creep was done by Liu et al. [76] for the transverse response of fiber reinforced composites using the Sokolovsky-Perzyna elastoviscoplastic model, the 3D FEM framework and the Newton–Raphson linearization method. Perfect bonding was assumed for the interface between the matrix and fibers. The viscoelastic response of a unidirectional fiber reinforced composite was studied by Katouzian et al. [77] by employing the FEM. The model predictions of creep strains were compared with the experimental data.

Thus, we agree with the conclusion made recently in [78] that, up to now, micromechanical lifetime prediction studies of unidirectional fiber reinforced composites at the conditions of high temperature creep, damage growth and material tension-compression asymmetry do not exist in the literature.

2. Experimental data

The introduction of titanium matrix composites (TMCs) into industrial applications was closely related to the experimental investigations of their mechanical properties, in particular, by National Aeronautics and Space Administration (NASA) and German Aerospace Center (DLR). Unfortunately, useful information about their mechanical properties is scattered in the literature [79].

2.1. Stresses and damage

In the present report, we take into account that *multiaxial stress states* in turbine blades made of *silicon carbide fiber reinforced TMCs* can be generated due to the thermal loads, as well as, due to centrifugal forces. Special attention is paid to the experimental data obtained at the DLR [4, 80, 81]. Hence, in order to study the degradation of composites, which may occur in-service up to 550 °C and limit the performance of turbine blades, the test specimens were subjected in the DLR laboratory to conditions, which simulate the in-service condition as close as

possible. The composite material was processed by deposition of the matrix alloy on the silicon carbide fibers using the magnetron sputtering process. The near-alpha titanium alloy Ti-6242 was used as matrix material. Its nominal composition is Ti–6%Al–2%Sn–4%Zr–2%Mo–0.1%Si (wt. %). The SiC fiber SCS-6 was used as long fiber reinforcement. The fiber is covered with a protection layer, which consists mainly of carbon. Testing in the DLR laboratory realizes cyclic thermal (Fig. 1) and mechanical loading in the axial direction of the sample. A heating period t_1, a dwell time $t_2 - t_1$ and a cooling period $t_3 - t_2$ in the applied test cycle should be introduced in order to represent the degradation of composite during an entire flight of a jet engine.

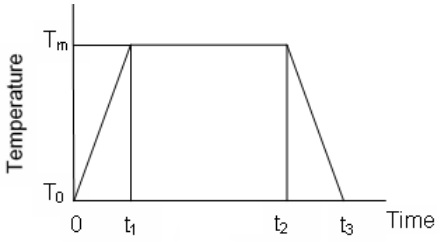

Fig. 1.The cycle of temperature

An applied axial tensile loading reproduces the centrifugal force acting on the turbine blade. In general, the temperature *T* and the load can act over time under an in-phase and out-of-phase loading mode (Fig. 2).

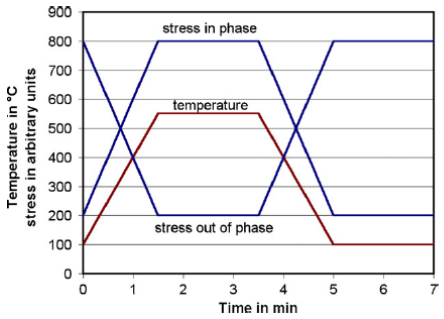

Fig. 2. Schematic representation of thermomechanical cyclic loading [80]

It was found [80] that out-of-phase thermomechanical loading generally leads to a stronger reduction in fatigue life than in-phase loading. This seems to be controlled by matrix cracking whereas failure during in-phase cycling appears to be dominated by fiber failure.

Also, the mechanical properties of TMCs were studied intensively by NASA [82]. In this regard, the unidirectional fiber-reinforced composite SCS-6/Ti-2411 was considered. This is a TMC manufactured using the titanium alloy Ti-2411 (Ti-24Al-11Nb) and silicon carbide-based fibers SCS-6 with carbon-rich coating layers. The shear strength of the SCS-6/Ti-2411 interface was investigated using fiber push-out test method (Fig. 3). In this way, it was possible to measure the relative fiber/matrix displacements at room temperature related to fiber sliding and interface debonding [82]. In the following, the single fiber fragmentation test method was developed in [83] to study the interfacial shear characteristics of Ti/SiC composites at elevated temperature.

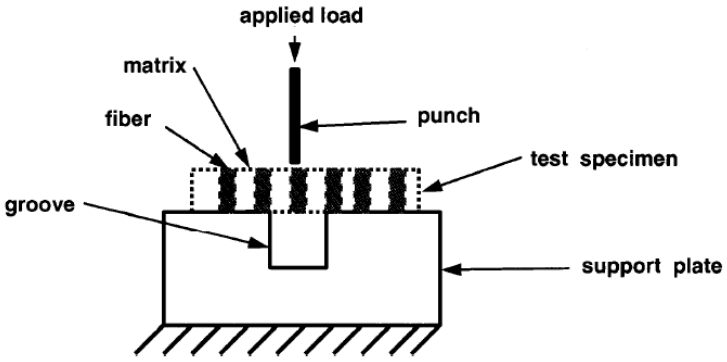

Fig. 3. Schematic representation of fiber push-out test method [82]

Obviously that initiation and growth of damage is closely related to the stress state in unidirectional fiber reinforced TMCs at the conditions of creep and fatigue with multiaxial stress state under thermomechanical cyclic loading. On the other hand, development of structural defects (vacancies, dislocations, pores, voids, microcracks, foreign atoms, grain boundaries, interfaces between fiber and matrix) with temperature and time will also change the distribution and magnitude of the residual stresses (thermal stresses, phase transformation stresses) that occur after manufacturing processing.

There are various sources of the operation induced stresses in TMCs:

a) Thermal induced stresses resulting from temperature changes and differences of the coefficient of thermal expansion of composite constituents.

b) Intrinsic growth stresses due to oxidation, chemical reactions, phase transformations, etc.

c) Stresses due to the deformation and damage development under the applied loading and environmental influences.

The consideration of the residual stresses in TMCs is quite important in the structural analysis of the system. However, this is not enough in order to understand the mechanisms of composite degradation over time that affect essentially the lifetime reduction of turbine blades at high temperatures. Therefore, it is necessary to identify the time dependent phenomena related to the thermal, chemical, mechanical and structural degradation of TMCs at high temperatures over time. These time dependent phenomena can be investigated experimentally. The phenomena under consideration are creep, fatigue, oxidation and phase transformation.

2.2. Creep

Titanium alloys at high temperatures exhibit creep deformation considered as a time-dependent irreversible deformation process. Even in the initial stages of the creep process in titanium alloys, dislocations, impurity atoms and voids accumulate at the grain boundaries to form grain boundary cavitation. As microscopic cavities at the grain boundaries get larger and coalesce, dislocations, impurity atoms and voids move out to grain boundaries, and micro-cracks along the grain facets begin to be formed. Growth and coalescence of these microcracks leads to the creep rupture in the final stage of the creep process with the formation of macrocracks with some preferential orientation, often, direction perpendicular to the maximum principal stress. Thus, creep deformation changes the microstructure of the titanium alloys by introducing dislocations, impurity atoms and voids in the initial stages, microscopic cavities in the following, and microcracks in the final stage of the creep process, all of them, at the grain boundaries with some preferential orientation. Furthermore, the velocity of the growth of already existing grain boundary microscopic cavities and microcracks, and of the nucleation of new ones essentially depends on the intensity of creep deformation. On the other hand, creep deformation of titanium alloys is influenced by the growth of microscopic cavities and microcracks. This influence begins at the primary and secondary stages of the creep process, and can be visible in the tertiary stage due to increase of the creep strain rate, preceding the creep rupture. The creep rupture case without increase in the creep strain rate can also be observed in titanium alloys.

Thus, creep deformation and material deterioration in titanium alloys due to growth of creep damage occur parallel to each other, and they have a reciprocal effect. Obviously that creep damage growth in the matrix leads to the degradation of titanium matrix composite over time.

A schematic of typical creep curves for MMCs with continuous and discontinuous reinforcement is shown in Fig. 4. It is stated [1] that composites with continuous fibers exhibit a short primary creep regime, followed by a long steady-state regime. However, the creep curves of continuously reinforced unidirectional titanium matrix composites exhibit in the tests in the longitudinal and transverse directions a short tertiary creep stage before rupture [80, 84].

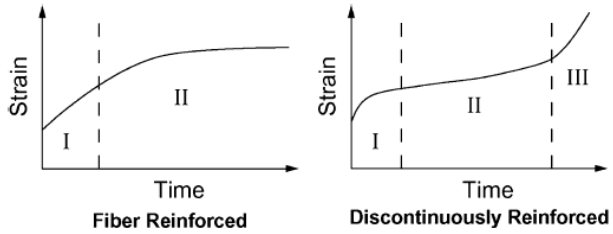

Fig. 4. Schematic of creep strain versus time for fiber reinforced and discontinuously reinforced MMCs [1]

Figure 5a shows the creep behavior of the Ti-6242 alloy in the temperature interval from 450 to 550 °C. The creep behavior of this titanium alloy at 500 °C is also discussed in [84]. Figure 5b demonstrates the creep behavior of a unidirectional SCS-6/ Ti-6242 composite at 550 °C under tension in the longitudinal direction. The creep rupture data for this composite are shown in Fig. 5c.

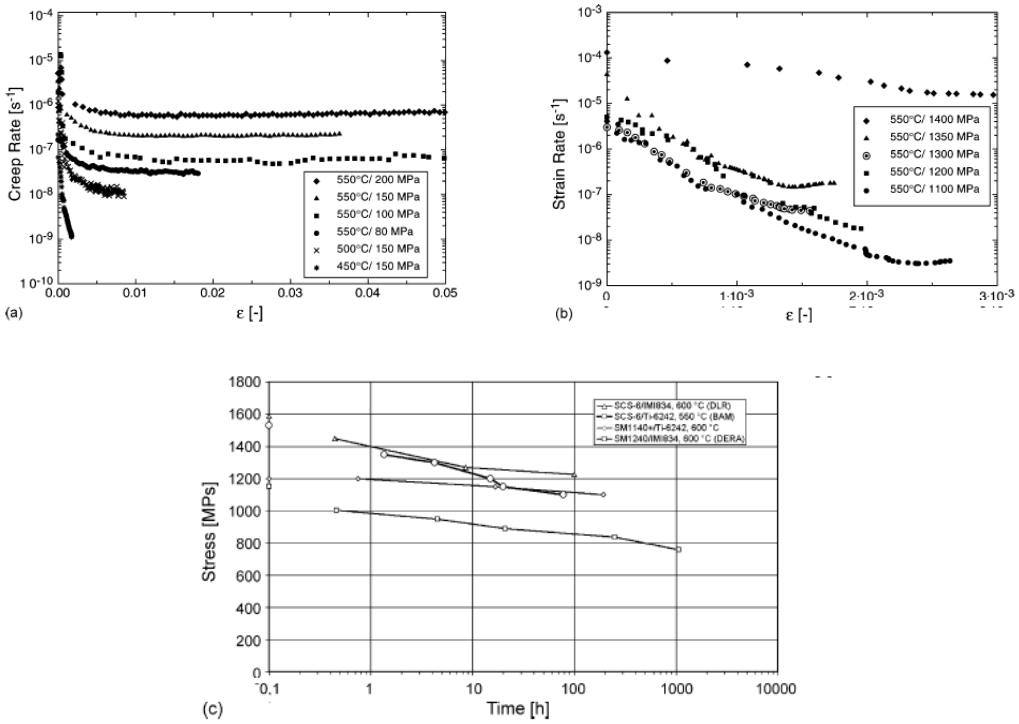

Fig. 5. (a) Creep rate vs. creep strain for Ti-6242 alloy; (b) Creep rate vs. creep strain for SCS-6 /Ti-6242 composite; (c)Tensile stress vs. time to fracture for titanium matrix composite [80]

The comparison of the longitudinal and transverse creep curves at 500 °C for a unidirectional SM1140+/Ti-6242 composite is presented in [84]. Results of the creep tests up to rupture in tension for SM1140+/Ti-6242 composite are given in Table 1. Creep tests clearly demonstrate that the composite under study is more creep resistant in the longitudinal direction than in the transverse direction due to the weak nature of matrix-fiber interfacial bond and week interfacial diffusion.

Table. 1. Experimental creep rupture data at 500 °C for SM1140+/Ti-6242 composite [84]

Fibre direction	Applied stress (MPa)	Rupture life (h)	Rupture creep strain (%)
0°	943	45 IT	0.08[a]
	1051	92 IT	0.07[a]
	1069	315 IT	0.14[a]
	1098	193	0.13
	1152	16.7	0.08
	1202	0.68	–
90°	150	1000 IT	0.073[a]
	250	400 IT	0.16[a]
	270	1000 IT	0.45[a]
	300	240	0.38
	320	200	0.44

IT: interrupted test.
[a] The reported value for an interrupted test is the creep strain at the end of the test.

Mechanisms leading to the creep rupture of the TMC can be summarized as follows [84].

1) **Longitudinal loading.** The stress relaxation in the matrix increases the load borne by the fibers. Thus, fibers breaks are thus produced during the creep deformation. Those fibers breaks induce stress concentrations on the neighboring fibers. Therefore, final creep rupture of the composite results from the accumulation of fiber fractures.

2) **Transverse loading.** The matrix controls the global creep deformation of the composite, but the load carried locally by the matrix is controlled by the strength of the interface. For low applied stresses (inferior to the critical stress), interfaces remain partially damaged, and load is sharing between the fibers. For high applied stresses (greater than the critical stress) all the interfaces are broken, and the load is totally carried by the matrix. The localization of the stress in the matrix induces the creep rupture of the composite.

In the following, a comparative analysis of the creep damage mechanisms under transverse loading has been given for the two unidirectional TMCs (SCS-6 /Ti-6242 and SM1140+/Ti-6242) [85].

In order to reproduce correctly the creep deformation in the transverse direction of the composite using the creep constitutive model it is necessary to take into account the anisotropic creep properties of the titanium alloy induced by the matrix texture. For example, the experimental data obtained on the samples taken in different directions of a Ti–6Al–4V plate demonstrate the initial anisotropy of creep [86, 87]. So, the rupture time of the longitudinal samples is less by a factor of 30 than one obtained on the transverse samples for one and the same value of the tensile stress in the creep experiments.

Also, Fig. 6a, b shows that the titanium alloy Ti-6242 [88] belongs to the broad class of structural materials [14, 23, 89-109] with different stress-strain diagrams in tension and compression.

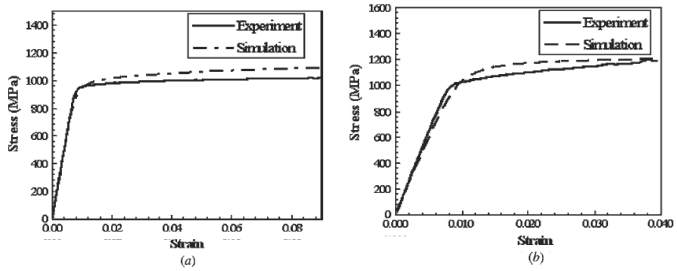

Fig. 6. Stress- strain diagram for Ti-6242 at room temperature under tension (a) and compression (b) [88]

Additionally, Fig. 7a, b shows different creep properties of the Ti-6242 alloy [88] in tension and compression. The difference in the durations before rupture of the Ti–6Al–4V samples under tension and compression reaches several orders of magnitude [86, 87]. Thus, titanium matrixes like many structural materials [9, 14, 23, 110-140] demonstrate different creep behavior under tensile and compressive loading types at the same temperature and for one and the same absolute value of the stress. In general, the tension/ compression asymmetry of the titanium alloys is a characteristic feature of the deformation behavior of light alloys [141]. Additionally note that the silicon-based materials also show different mechanical responses under tension and compression [142].

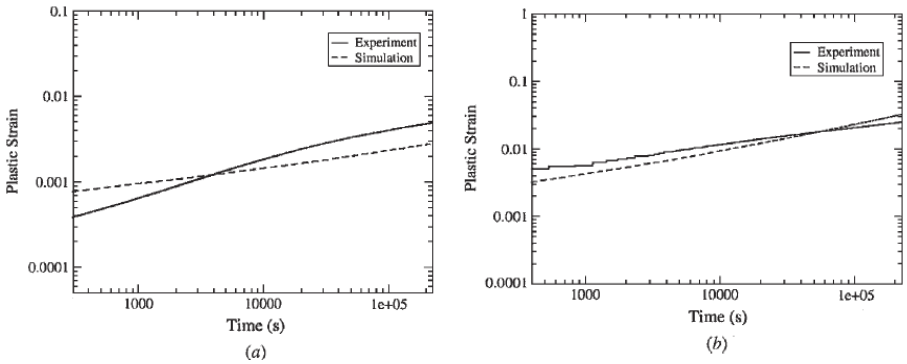

Fig. 7. Time-dependent behavior of Ti-6242 alloy at room temperature under compression with 907 MPa (a) and under tension with 897 MPa (b) [88]

As a conclusion, it is necessary to take into account simultaneously the initial anisotropy and tension/ compression asymmetry of the matrix material during the constitutive modeling of unidirectional fiber reinforced TMCs under multiaxial loading, as well as, to modify a number of the well-known constitutive models [143-155] towards the consideration of the effect of the kind of loading on the anisotropic time-dependent material behavior.

2.3. Fatigue

The TMCs used at high temperature in aerospace applications are subjected to cyclic mechanical loading as well as periodic temperature variation during the start-up and shut-down of the engine, which gives rise to the so-called

thermomechanical fatigue (TMF) and life limitation of the components. In many cases isothermal low cycle fatigue (LCF) tests were used to evaluate the TMF life because of expensive equipment and time-consumption for TMF test. Therefore, it is necessary to clarify TMF behaviors of TMCs under the simulated service conditions in the laboratory for the safety and reliability of the used materials.

The LCF tests at 550°C and the TMF tests with temperature cycles between 100°C and 550°C for a unidirectional SCS-6/ Ti-6242 composite were conducted at the DLR [4, 80, 81]. The TMF behavior of the composite was studied either in-phase (IP) or out-of-phase (OP) (Fig. 8). The fatigue life data for SCS-6/ Ti-6242 composite are presented in Fig. 8. It is seen that at the same temperature portion, the fatigue life under IP mode is much longer than OP mode. Under OP mode, the high tensile stress at minimum temperature acts on the specimen, and fatigue microcracks can easily nucleate. In contrast to this, the tensile stress is lowered in IP condition because of the significant improvement of the deformability of the alloy at the high temperature. As a result, the fatigue microcrack initiation is delayed under IP mode.

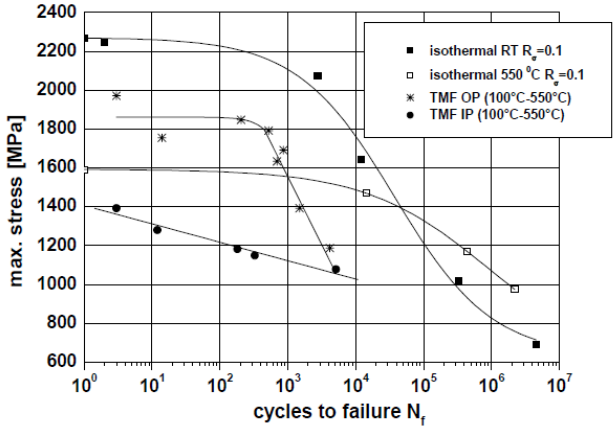

Fig. 8. Isothermal and thermomechanical fatigue life for SCS-6/Ti-6242 (fiber content V_f=0.35) [80]

Cyclic tension-compression loading (stress ratio R <0) of TMCs differs from the tension-tension loading [156]. Once the microcracks are initiated, they open (*damage growth*) and close (*damage healing*) periodically. This leads to friction in the fiber-matrix interface, and shear stresses in the bridging fibers due to microscopic mismatch of the microcracks while closing, resulting in a reduction of fiber strength and rapid failure of the composite. The fracture surfaces of specimens tested under tension-tension and tension-compression loading are shown in Fig. 9. It is seen that *the fatigue life strongly depends on the mean stress as well as on the loading mode*. In the tension-tension mode the opened matrix microcrack induces shear failure of the fiber-matrix interface, and thus, fiber breakage occurs at the weakest location within the debonded length. Under tension-compression loading the same debonding mechanisms occur. However, the fibers do not fail at their weakest point within the debonded length but are weakened by friction and shear forces in the region of the matrix microcracks. The fracture surfaces of fibers and matrix are nearly in the same plane resulting in an apparent shorter debonded length. Even so it can be assumed that the debonding mechanism is similar in both cases, since the mechanisms of load sharing and fiber-matrix load transfer are depending on the materials properties and not on the loading conditions.

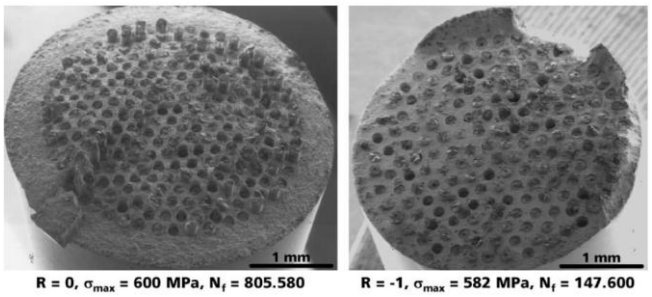

Fig. 9. Comparison of the fracture surfaces for TMC under tension-tension loading (left) and tension-compression loading (right) [156]

The TMF tests for SCS-6/ Ti-6242 composite are conducted in [157] under stress control using a stress ratio R of zero and a temperature cycle between 100 and 450°C. It is seen (Fig.10) that ratcheting occurs in the composite due to the cyclic softening of the matrix material.

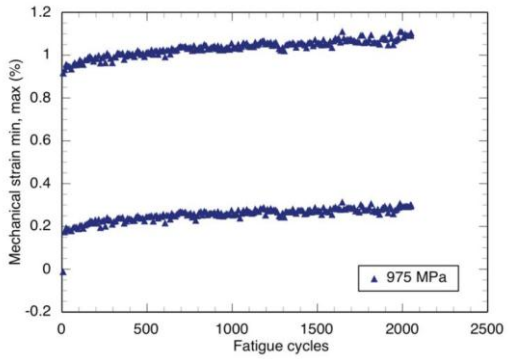

Fig. 10. Maximum and minimum mechanical strain as a function of the TMF cycles [157]

Tension–tension fatigue properties of a SiC fiber reinforced TMC were studied at room temperature [158]. Matrix cracking, fiber/matrix interface debonding and fiber pull-out phenomenon were observed.

In order to describe the fatigue damage evolution and ratcheting in SCS-6/ Ti-6242 composite using the constitutive model it is necessary to have the experimental data for titanium alloy Ti-6242. The fatigue life data for Ti-6242 alloys of different microstructure [159] are presented in Fig. 11.

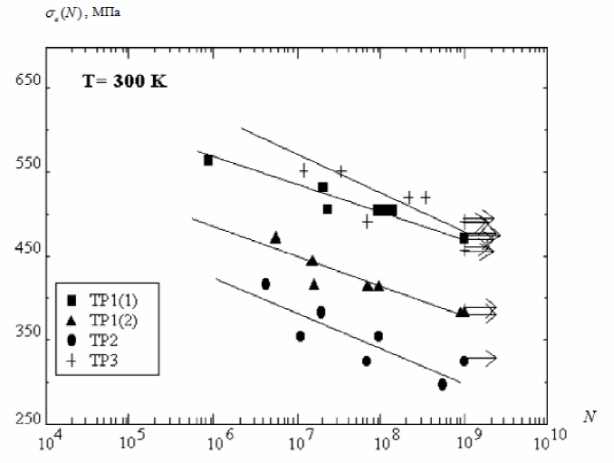

Fig. 11. Stress amplitude as a function of cycles to failure for Ti-6242 alloys of different microstructure (TP1, TP2, TP3) at room temperature [159]

The LCF tests at 350°C for Ti-6242 alloy were conducted with the applied total strain range Δε= 1.2% and with the strain ratio $R_\varepsilon = \varepsilon_{\min} / \varepsilon_{\max}$ =0 and 0.6 [160]. Quick decreasing of maximum and minimum stresses with number of cycles occurs at the fixed temperature before failure (Fig. 12). This is the combined action of ratcheting and fatigue damage accumulation in these experiments.

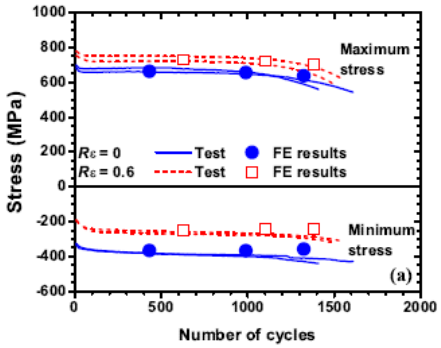

Fig. 12. Development of maximum and minimum stress with cycle number for Ti-6242 at 350°C [160]

The LCF tests at different fixed temperatures for Ti-6242 alloy were conducted with the applied strain range Δε/2= 0.7% and with the strain ratio R_ε = -1 [161]. Quick decreasing of the stress amplitude with number of cycles occurs before failure (Fig. 13). This effect can be explained by the combined action of ratcheting and fatigue damage growth.

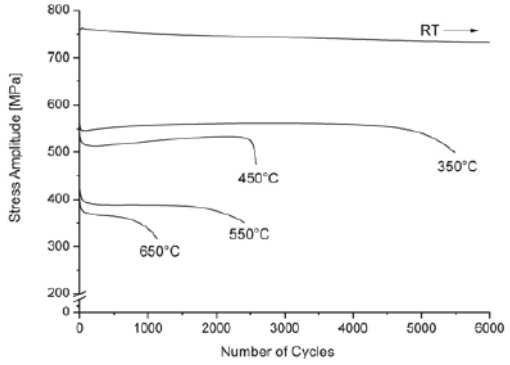

Fig. 13. Development of the amplitude stress with cycle number for Ti-6242 with Δε/2= 0.7% and R_ε = -1 [161]

2.4. Phase transformation

The matrix material Ti-6242 belongs to the near-α titanium alloys which combine the good creep resistance of α -alloys with the high strength of ($\alpha + \beta$)-alloys. The formation of the α phase, its morphology, volume fraction, size, distribution is influenced by the phase transformation kinetics during heat treatments [162,163]. The microstructure of Ti-6242 can be manipulated by changing the solution-annealing temperature to below the β -transus (T_β). The α - morphology is also influenced by the cooling rate. In this regard, specimens were solution annealed at various temperatures below T_β to control the volume fraction of primary α -phase and were subsequently shot-peened [164]. The influence of the changes in primary α - phase on the low-cycle dwell-time fatigue (LCDF) life was determined and compared to the conventional LCF properties of the Ti-6242 alloy. The increasing primary α - phase associated with lower solution temperatures appears to increase susceptibility to LCDF (Fig. 14) and ratcheting. This effect may be related to the nucleation mechanism involving an association of transgranular microcracks with slip across the α - grains [164].

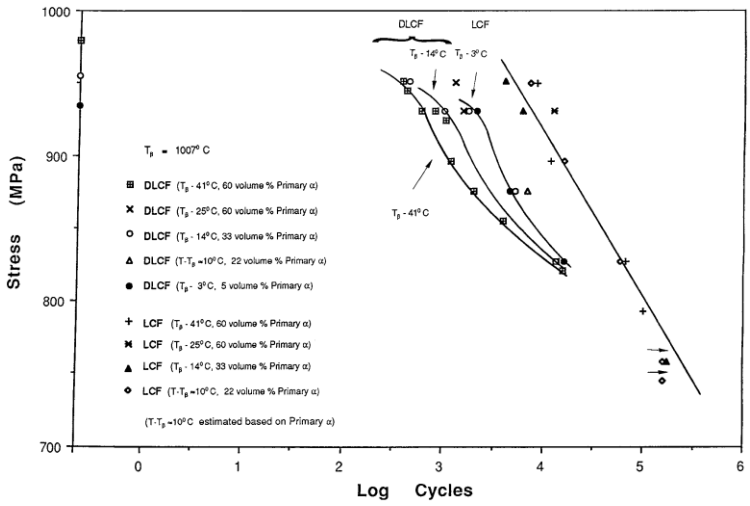

Fig. 14. Dwell- and low-cycle fatigue data for Ti-6242 where the reported stress is the peak stress and the minimum stress is zero [164]

2.5. Oxidation

Oxidation of the carbon protective coating in SCS-6/ Ti-6242 composite has been studied at temperatures of 400, 500 and 600 °C up to a maximum time of 800 h [165]. Weight loss and thickness reduction of the initial 3.5 μm thick protection layer is measured as a function of the time. Also, the influence of the oxidation on the strength of the fiber has been investigated experimentally. Thus, the chemical strain in the protective coating influenced by the oxidation, as well as, oxidation induced stresses and oxidation damage should be considered in the constitutive model in order to study mechanical response and damage evolution in TMCs at high temperatures.

Also, the oxidation of the protective coating was observed (Fig. 14) in the creep tests of a unidirectional fiber reinforced SCS-6/Ti-6Al-4V composite at temperatures from 427 to 650 °C and stresses from 621 to 1380 MPa [166]. The results indicate that oxidation damage in the protective coating and inefficient load transfer under creep conditions significantly decreased the capability of broken fibers to carry load.

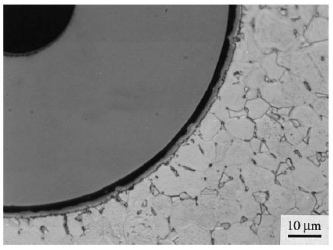

Fig. 15. SEM micrograph of oxidized protective coating in SCS-6/Ti-6Al-4V composite under creep conditions [166]

3. Constitutive modeling

Let $x_i\ (i=1,2,3)$ denote coordinates of a material point in the initial (undeformed) configuration of the composite constituents (matrix, reinforcement, interfaces and coating), while X_i are its coordinates in the deformed (current) configuration at a given instant of time $t\ (t\neq 0)$. Assume, for simplicity, that the initial configuration of the composite constituent and its current configuration are referred to the same coordinate frame $x_i\ (i=1,2,3)$.

In the Lagrangian formulation of the constitutive model at finite strains it is necessary to introduce the Cauchy-Green strain tensor as an important strain measure in the reference configuration of the composite constituent in the following form [167]:

$$\varepsilon_{ij}=0.5\left(u_{i,j}+u_{j,i}+u_{k,i}u_{k,j}\right), \tag{1}$$

where $u_i(x_1,x_2,x_3,t)=X_i-x_i$ are the components of the displacement vector of the material points at time t in directions x_1,x_2,x_3, respectively. It is not difficult to obtain the material time derivative of the Cauchy-Green strain tensor

$$\dot{\varepsilon}_{ij}=0.5\left(\dot{u}_{i,j}+\dot{u}_{j,i}+u_{k,i}\dot{u}_{k,j}+u_{k,j}\dot{u}_{k,i}\right),(i,j,k=1,2,3), \tag{2}$$

where the dot above the symbol denotes a material time derivative. The rate of strain tensor in the current configuration of the composite constituent can be defined as follows [167]:

$$d_{ij}=0.5\left(\frac{\partial\dot{u}_i}{\partial X_j}+\frac{\partial\dot{u}_j}{\partial X_i}\right). \tag{3}$$

The connection between $\dot{\varepsilon}_{ij}$ and d_{ij} has a form [167]:

$$\dot{\varepsilon}_{ij}=\frac{\partial X_k}{\partial x_i}\frac{\partial X_l}{\partial x_j}d_{kl} \tag{4}$$

or

$$d_{ij}=\frac{\partial x_k}{\partial X_i}\frac{\partial x_l}{\partial X_j}\dot{\varepsilon}_{kl}. \tag{5}$$

Then the additive decomposition of the time derivative of the total Cauchy-Green strain tensor and of the rate of strain tensor acting on the current configuration of the composite constituent to a linear elastic part, nonlinear elastic part, plastic part, creep part and chemical one may be postulated, respectively, in the following form:

$$\dot{\varepsilon}_{ij} = \dot{\varepsilon}_{ij}^{e} + \dot{\varepsilon}_{ij}^{ne} + \dot{\varepsilon}_{ij}^{p} + \dot{\varepsilon}_{ij}^{c} + \dot{\varepsilon}_{ij}^{s} \tag{6}$$

and

$$d_{ij} = d_{ij}^{e} + d_{ij}^{ne} + d_{ij}^{p} + d_{ij}^{c} + d_{ij}^{s}. \tag{7}$$

The second Piola-Kirchhoff stress tensor τ_{ij} in the composite constituent can be expressed in term of the Cauchy stress tensor σ_{ij} as follows [167]

$$\tau_{ij} = J\sigma_{kl}\frac{\partial x_i}{\partial X_k}\frac{\partial x_j}{\partial X_l} \tag{8}$$

and

$$\sigma_{ij} = J^{-1}\tau_{kl}\frac{\partial X_i}{\partial x_k}\frac{\partial X_j}{\partial x_l}, \tag{9}$$

where J is the Jacobian of deformation; $\mathbf{F}$ is the matrix of the deformation gradients in the current configuration at time t; $J = \det\mathbf{F}$; $\mathbf{F} = \left[\frac{\partial X_i}{\partial x_j}\right] = \left[\delta_{ij} + u_{i,j}\right], (i,j = 1,2,3)$; δ_{ij} is the Kronecker delta.

Now we introduce objective stress rate, such as, the Truesdell derivative $\sigma_{kl}^{\mathrm{Tr}}$ of the Cauchy stress tensor which is essential in order to formulate the constitutive equations for the mechanical response of the composite constituent in the rate form. Note also that the material time derivative of the Cauchy stress tensor σ_{kl}, i.e. $\dot{\sigma}_{kl}$, is affected by rigid-body motions, and it is not objective (not frame-indifferent) [167]. The Truesdell derivative of the Cauchy stress tensor and the material derivative of the second Piola-Kirchhoff stress tensor are connected by the relation [167]:

$$\dot{\tau}_{ij} = J\sigma_{kl}^{\mathrm{Tr}}\frac{\partial x_i}{\partial X_k}\frac{\partial x_j}{\partial X_l}, \tag{10}$$

which is similar to Eq. (8). Then the relation between $\sigma_{kl}^{\mathrm{Tr}}$ and d_{ij}^{e} will be accepted in such a form

$$\sigma_{kl}^{\mathrm{Tr}} = A_{klrs}^{*}\left(d_{rs} - d_{rs}^{ne} - d_{rs}^{p} - d_{rs}^{c} - d_{rs}^{s}\right). \tag{11}$$

Here A_{klrs}^{*} is the symmetrical tensor of the appropriate elastic constants in the generalized Hooke's law. By substituting Eq. (11) into Eq. (10) and then taking into account Eq. (5) we obtain

$$\dot{\tau}_{ij} = A_{ijkl}\left(\dot{\varepsilon}_{kl} - \dot{\varepsilon}_{kl}^{ne} - \dot{\varepsilon}_{kl}^{p} - \dot{\varepsilon}_{kl}^{c} - \dot{\varepsilon}_{kl}^{s}\right), \tag{12}$$

where

$$A_{ijkl} = JA_{mnrs}^{*}\frac{\partial x_i}{\partial X_m}\frac{\partial x_j}{\partial X_n}\frac{\partial x_k}{\partial X_r}\frac{\partial x_l}{\partial X_s}\left(m,n,r,s = 1,2,3\right). \tag{13}$$

It is not difficult to establish that condition $A_{ijkl} = A_{klij}$ of symmetry is valid.

Considering the composite constituent, in general, as the anisotropic material with different behavior in tension and compression, the connection between the kinematic tensor e_{kl} in the current configuration and the Kirchhoff stress tensor T_{kl} can be written as follows [9, 11, 12, 111]:

$$e_{ij} = e_0\left(\frac{a_{ijkl}T_{kl}}{T_2} + b_{ij}\right). \tag{14}$$

Here $T_{kl} = J\sigma_{kl}$; $e_0T_e = T_{ij}e_{ij}$; $T_e = T_1 + T_2$; $T_1 = b_{ij}T_{ij}$; $T_2^2 = a_{ijkl}T_{ij}T_{kl}$; b_{ij} and a_{ijkl} are the second order and fourth order material tensors; T_1 and T_2^2 are the linear and quadratic joint invariants of the Kirchhoff stress and the material tensors; T_e is the equivalent Kirchhoff stress; e_0 is the scalar function which depends on T_e, as well as, some structural parameters, and which specifies for each physical state of the composite constituent (nonlinear elasticity, plasticity, creep). For example, such structural parameters can be the Kachanov-Rabotnov damage parameter ω [168, 169] reflecting the growth of damage, and the healing parameter h [170-173] describing the healing of damage affected by loading and environmental factors. Thus, e_0 is some function of T_e, ω and h. Damage

parameter is increasing with time from the initial value $\omega = \omega_0$ at the reference instant to the final value $\omega = \omega_*$ at the instant of rupture. In the simplest case it is possible to accept that $\omega_0 = 0$ and $\omega_* = 1$. Also, the healing parameter is increasing with time from the initial value $h = h_0$ at the reference instant to the final value $h = h_*$. In the simplest case we can accept that $h_0 = 0$ and $h_* = 1$.

In the case of the nonlinear elasticity, the kinematic tensor $e_{kl} \equiv d_{kl}^{ne}$ is the nonlinear elastic part of the rate of strain tensor in the current configuration, and it is necessary to specify e_0 as some function of T_e, ω, and h to reflect damage growth, deformation hardening and deformation softening in the composite constituents under nonlinear elastic deformation.

For plastic deformation of the composite constituent, the kinematic tensor $e_{kl} \equiv d_{kl}^{p}$ in Eq. (14) is the plastic part of the rate of strain tensor in the current configuration, and it is necessary to define the conditions when $d_{kl}^{p} = 0$ in the cases of elastic deformation, of unloading or neutral loading, as well as, the condition of loading.

Considering creep deformation of the composite constituents, it is possible to assume that the kinematic tensor $e_{kl} \equiv d_{kl}^{c}$ in Eq. (14) is the creep part of the rate of strain tensor in the current configuration, and the scalar multiplier in Eq. (14), for example, in the case without healing of damage can be defined as

$$e_0 = \frac{v(T_e)\,\omega^r}{\left(1-\omega^{-r+1}\right)^m}. \tag{15}$$

Different examples on how to specify function $v(T_e)$ and creep damage evolution equation for ω are given in [14, 23, 174].

For orthotropic materials with coincidence of the coordinate axes with the principal directions of anisotropy Eq. (14) takes the following form [9, 11, 12, 111]:

$$e_{11} = e_0\left(\frac{a_{1111}T_{11} + a_{1122}T_{22} + a_{1133}T_{33}}{T_2} + b_{11}\right), \quad e_{12} = 2e_0\,\frac{a_{1212}T_{12}}{T_2} \quad (1, 2, 3). \tag{16}$$

Here the symbol (1, 2, 3) means that the rest of the relations can be obtained from Eq. (16) by circular transposition of lower indexes 1, 2 and 3;

$$T_2^2 = a_{1111}T_{11}^2 + a_{2222}T_{22}^2 + a_{3333}T_{33}^2 + 2a_{1122}T_{11}T_{22} + 2a_{1133}T_{11}T_{33} + 2a_{2233}T_{22}T_{33} + 4a_{1212}T_{12}^2 + 4a_{1313}T_{13}^2 + 4a_{2323}T_{23}^2,$$

$$T_1 = b_{11}T_{11} + b_{22}T_{22} + b_{33}T_{33}. \tag{17}$$

Further simplification of Eqs. (16), (17) for orthotropic materials when the coordinate axes coincide with the principal directions of anisotropy is related to the following requirements [175,176]

$$a_{1111} = a_{11}^2,\ 2a_{1122} = -a_{11}a_{22},\ 4a_{1212} = 3a_{11}a_{22} + a_{12}^2 \ (1, 2, 3) \tag{18}$$

using the six material parameters a_{11}, a_{22}, a_{33}, a_{12}, a_{23} and a_{13}. Then it is easy to obtain from Eqs. (16)-(18) the following tensor connection [176]

$$e_{11} = e_0\left[\frac{a_{11}^2T_{11} - \frac{1}{2}\left(a_{11}a_{22}T_{22} + a_{11}a_{33}T_{33}\right)}{T_2} + b_{11}\right], \qquad e_{12} = \frac{1}{2}e_0\,\frac{\left(3a_{11}a_{22} + a_{12}^2\right)T_{12}}{T_2} \quad (1, 2, 3), \tag{19}$$

where $T_2^2 = a_{11}^2T_{11}^2 + a_{22}^2T_{22}^2 + a_{33}^2T_{33}^2 - a_{11}a_{22}T_{11}T_{22} - a_{11}a_{33}T_{11}T_{33} - a_{22}a_{33}T_{22}T_{33} + \left(3a_{11}a_{22} + a_{12}^2\right)T_{12}^2 + \left(3a_{11}a_{33} + a_{13}^2\right)T_{13}^2 + \left(3a_{22}a_{33} + a_{23}^2\right)T_{23}^2$.

Another possible simplification of Eqs. (16), (17) for orthotropic materials with coincidence of the coordinate axes with the principal directions of anisotropy is related to the requirements [177] $a_{1111} = G_0 + H_0$, $a_{2222} = F_0 + H_0, a_{3333} = G_0 + F_0, a_{1122} = -H_0, a_{2233} = -F_0, a_{1133} = -G_0, 2a_{1212} = N_0, 2a_{2323} = L_0, 2a_{1313} = M_0$, based on the six material parameters G_0, H_0, F_0, N_0, L_0 and M_0. Then the equivalent Kirchhoff stress has a form

$$T_e = T_1 + \sqrt{H_0\left(T_{11}-T_{22}\right)^2 + F_0\left(T_{22}-T_{33}\right)^2 + G_0\left(T_{33}-T_{11}\right)^2 + 2N_0T_{12}^2 + 2L_0T_{23}^2 + 2M_0T_{13}^2}. \tag{20}$$

In a particular case of the transverse isotropy with a single axis of symmetry 1 the following equalities in Eqs. (16), (17) take place $b_{22} = b_{33}, a_{2222} = a_{3333}$, $a_{1122} = a_{1133}$, $a_{1212} = a_{1313}, a_{2222} = 2a_{2323} + a_{2233}$.

For composite constituents with the initial isotropy of mechanical properties it is necessary to accept in Eqs. (16), (17) the conditions, such that $b_{11}=b_{22}=b_{33}, a_{1111}=a_{2222}=a_{3333}$, $a_{1122}=a_{1133}=a_{2233}, a_{1212}=a_{1313}=a_{2323}$, $a_{1111}=2a_{1212}+a_{1122}$.

Remark 1. Using the spin tensor $\Omega_{ij}=0.5\left(\frac{\partial \dot{u}_i}{\partial X_j}-\frac{\partial \dot{u}_j}{\partial X_i}\right)$ and the Jaumann stress derivative [167] $\sigma_{ij}^{\mathrm{J}}=\dot{\sigma}_{ij}-\Omega_{ir}\sigma_{rj}+\sigma_{ir}\Omega_{rj}$ instead of the Truesdell stress derivative in Eq. (11) does not provide satisfaction of the symmetry condition $A_{ijkl}=A_{klij}$.

Remark 2. As mentioned recently [178], up to now there is nothing more fundamental in nonlinear mechanics of anisotropic materials with tension-compression asymmetry than the constitutive framework [9, 11, 12, 111] developed in the early 1980s.

Remark 3. The model under discussion was used intensively by researchers in Ukraine [179, 180], Russia [181-184], Japan [185, 186], South Korea [187-189], China [190-193], Switzerland [194-198], UK [199-201] and USA [202, 203], however, *without referencing the original sources* [9, 11, 12, 111].

Remark 4. The present model reflects in a particular case the characteristic features of the anisotropic bimodular materials [10-12, 22, 204-210].

Remark 5. The chemical part of the rate of strain tensor in the current configuration of the composite constituent can be defined using Fick's second law of diffusion [120, 123, 211-217].

Remark 6. Procedure for the identification of material parameters in the constitutive equations has been developed in [218-220].

Remark 7. The constitutive model under discussion can be extended to the case of the anisotropic creep hardening under nonproportional loading according to the approaches [221, 222]. Formulations of the kinetic equations for fatigue damage in the composite constituents are given in [223-234].

4. Numerical modeling and simulation

Two different arrangements of fibers are considered for numerical calculations of multiaxial stresses and damage in the unidirectional TMCs subjected to thermomechanical loading under creep conditions, namely, rectangular and hexagonal arrangements. In this regard, two types of the unit cells (Figs. 16 a, b) are taken into account with periodic boundary conditions.

In the first case (Fig. 16 a) we take into the consideration three composite constituents, i.e., the fiber, protective coating and matrix, as well as, two distinct interfaces, one between the fiber and coating and the other between coating and matrix. Also, the other RVE (Fig. 16 b) has to be considered.

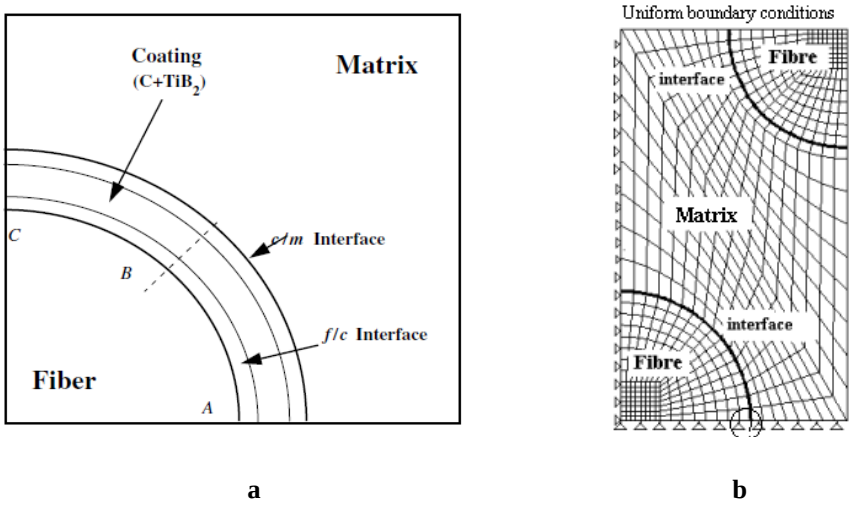

a **b**

Fig. 16. The RVE for rectangular (a) and hexagonal (b) arrangements of fibers in TMCs with details of composite constituents [84, 85]

Analysis of stress distributions over time in TMCs, damage analysis and lifetime prediction studies of composites are related to the consideration of the nonlinear initial/ boundary value multiphysics problem [174, 235, 236]. The Lagrangian variational functional for this problem at finite strains can be written in such a form [23]:

$$\Lambda(\dot{u}_i) = 0.5\iiint_{\Omega}\left[A_{ijkl}\left(\dot{\varepsilon}_{ij} - \dot{p}_{ij}\right)\left(\dot{\varepsilon}_{kl} - \dot{p}_{kl}\right) + \tau_{ij}\dot{u}_{k,i}\dot{u}_{k,j}\right]\mathrm{d}\Omega - \iint_{S_p}\dot{P}_i\dot{u}_i\mathrm{d}S \tag{21}$$

with

$$\dot{p}_{kl} = \dot{\varepsilon}_{kl}^{ne} + \dot{\varepsilon}_{kl}^{p} + \dot{\varepsilon}_{kl}^{c} + \dot{\varepsilon}_{kl}^{s} \tag{22}$$

Now, from the variational equation $\delta\Lambda = 0$ the linearized equation of equilibrium and natural boundary conditions, expressed in the terms of displacement rates, can be obtained as follows:

$$\left(\dot{\tau}_{kj}\left(\delta_{ik} + u_{i,k}\right) + \tau_{kj}\dot{u}_{i,k}\right)_{,j} = 0, \mathbf{x} \in \Omega \tag{23}$$

and

$$\left(\dot{\tau}_{kj}\left(\delta_{ik} + u_{i,k}\right) + \tau_{kj}\dot{u}_{i,k}\right)n_j = \dot{P}_i, \mathbf{x} \in S_p \tag{24}$$

Here, we assume that the TMC under consideration at an initial instant of time $t = 0$ occupies a finite region Ω in the three-dimensional Euclidean space. The surface $\partial\Omega$ of the region Ω is always assumed to be bounded, closed and partially smoothed one. The body is fixed on the part of surface S_u, and it is loaded by the surface force $\mathbf{P} = (P_1, P_2, P_3)$ per unit area of the undeformed surface S_p. Also, assume that the volume forces are absent.

The finite element models derived from Figs. 16 a, b may help to effectively simulate the influences of thermomechanical loading and environment on the micromechanical behavior of TMCs under high temperature and creep conditions. For this purpose, the constitutive framework given by Eqs. (12) and (14) needs to be incorporated into ABAQUS [174, 209], ANSYS [120, 214, 215, 217] and in-house developed software [238-241] in a form of the computer-based structural modeling tools. These software packages give the possibility to calculate the time dependent multiaxial stress distribution, as well as, changes of damage parameter at a discrete site of composite constituents under applied loading conditions as a function of the TMC parameters, environmental factors and composite functionality, and additionally to predict the lifetime of a TMC. It is established numerically that the titanium matrix controls the global deformation of the composite, while the interfaces control the load carried by the matrix. The observed interface damage is the interface debonding. Considering the interface damage evolution, it is possible to distinguish two main domains which define a critical stress (Fig. 17). The first domain (below the critical stress) is characterized by slight interface damage leading to a low creep rate for a long period of time [85]. The second domain (above the critical stress) related to a higher creep rate is characterized by appearance and propagation of the interface debonding leading to a creep rupture.

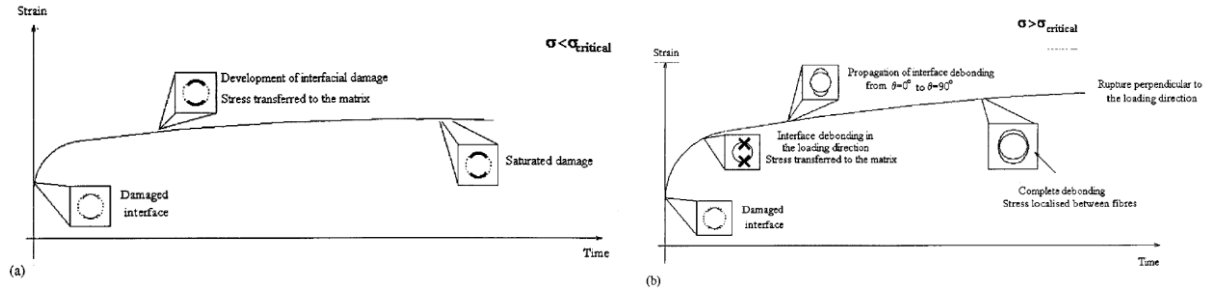

Fig. 17. Interface damage evolution: (a) below the critical stress, (b) above the critical stress [85]

5. Conclusion

Present report is a continuation of the author's review cycle [242-244] in the field of nonlinear solid mechanics for aerospace applications.

Also, this report was written during the 2022 russian military attacks on the Saltivka district, Kharkiv, Ukraine, using Tigrs, artillery shells, bombs and rockets [245].

References

1. Chawla, N., Chawla, K. K. (2013). Metal Matrix Composites. New York: Springer, Second Edition, 370p. DOI: 10.1007/978-1-4614-9548-2
2. Dadkhah, M., Saboori, A., Fino, P. (2019). An overview of the recent developments in metal matrix nanocomposites reinforced by graphene. Materials, 12(17), 2823-1–2823-38. DOI: 10.3390/ma12172823
3. Leyens, C., Hausmann, J., Kumpfert, J. (2003). Continuous fibre reinforced titanium matrix composites: Fabrication, properties and applications. In Leyens C., Peters M. (eds.), Titanium and Titanium Alloys (pp. 305-331). Weinheim: Wiley. DOI: 10.1002/3527602119.ch12
4. Figiel, Ł., Günther, B. (2008). Modelling the high-temperature longitudinal fatigue behaviour of metal matrix composites (SiC/Ti-6242): Nonlinear time-dependent matrix behaviour. International Journal of Fatigue, 30(2), 268-276. DOI: 10.1016/j.ijfatigue.2007.01.056
5. Zolochevsky, A. (2014). Stresses in novel layered materials induced by manufacturing: A review. Technical Report, Kharkiv: Research Center «Polytech», 20p. https://www.researchgate.net/publication/333632374
6. Borbély, A., Cloetens, P., Maire, E., Requena, G. (2011). Submicron tomography using high energy synchrotron radiation. In Lasagni F. A., Lasagni A. F. (eds.), Fabrication and Characterization in the Micro-Nano Range (pp. 151-170). Berlin: Springer. DOI: 10.1007/978-3-642-17782-8_7
7. Withers, P. J., Preuss, M. (2012). Fatigue and damage in structural materials studied by X-ray tomography. Annual Review of Materials Research, 42, 81-103. DOI: 10.1146/annurev-matsci-070511-155111
8. Zolochevsky, O., Konkin, V. (1992). Experimental research of nonlinear deformation and creep of rectangular plates and axisymmetrical shells. In Proceedings of the XV Symposium on Experimental Mechanics of Solids (pp. 256-258). Warsaw: Warsaw University of Technology. https://www.researchgate.net/publication/295179919
9. Zolochevskii, A. A. (1982). Allowance for differences in strain resistance in the creep of isotropic and anisotropic materials. Journal of Applied Mechanics and Technical Physics, 23(4), 591-596. DOI: 10.1007/BF00916729
10. Ambartsumian, S. A. (1982). Bimodulus Theory of Elasticity. M.: Nauka, 320p.
11. Zolochevskii, A. A. (1985). Tensor relationship in the theories of elasticity and plasticity of anisotropic composite materials with different tensile and compressive strength. Mechanics of Composite Materials, 21(1), 41-46. DOI: 10.1007/BF00611805
12. Zolochevskii, A. A. (1985). Determining equations and some problems of the variable-modulus theory of elasticity of anisotropic materials. Journal of Applied Mechanics and Technical Physics, 26(4), 572-578. DOI: 10.1007/BF01101644
13. Altenbach, H., Dankert, M., Zoločevskij, A. (1990). Anisotrope mathematisch-mechanische Modelle für Werkstoffe mit von der Belastung abhängigen Eigenschaften. Technische Mechanik, 11(1), 5-13. https://www.researchgate.net/profile/Alexander-Zolochevsky/publication/259737680
14. Altenbach, H., Altenbach, J., Zolochevsky, A. (1995). Erweiterte Deformationsmodelle und Versagenskriterien der Werkstoffmechanik. Stuttgart: Deutsher Verlag für Grundstoffindustrie, 172S. https://www.researchgate.net/publication/264895088
15. Zolochevsky, A. (1995). The formulation of constitutive equations for anisotropic materials with different behaviour in tension and compression. In Parker D. F., England A. H. (eds.), IUTAM Symposium on Anisotropy, Inhomogeneity and Nonlinearity in Solid Mechanics (pp. 351-356). Dordrecht: Springer. DOI: 10.1007/978-94-015-8494-4_48
16. Zolochevsky, A. (1996). The formulation of constitutive equations for fibre-reinforced composites with different behaviour in tension and compression. Mechanics Research Communications, 23(1), 55-60. DOI: 10.1016/0093-6413(95)00077-1
17. Zolochevsky, A. (1996). Identification of damage variable in ceramic matrix composite with different behaviour in tension and compression. In Fracture Mechanics of Ceramics, Vol. 12 (pp. 413-428). Boston: Springer. DOI: 10.1007/978-1-4615-5853-8_30
18. Zolochevsky, A. (1996). Damage analysis of ceramic composites with different behaviour in tension and compression. In Wang T., Chou T. W. (eds.), Progress in Advanced Materials and Mechanics, Vol. 1 (pp. 790-795). Beijing: Peking University Press. https://www.researchgate.net/publication/264623249
19. Voyiadjis, G. Z., Zolochevsky, A. (1998). Creep theory for transversely isotropic solids sustaining unilateral damage. Mechanics Research Communications, 3(25), 299-304. DOI: 10.1016/S0093-6413(98)00041-X
20. Betten, J., Zolochevska, L., Zolochevsky, A. (1999). Modelling of elastic deformation for initially anisotropic materials sustaining unilateral damage. Technische Mechanik, 19(3), 211-222. https://www.researchgate.net/publication/259723303
21. Mahnken, R. (2003). Creep simulation of asymmetric effects by use of stress mode dependent weighting

functions. International Journal of Solids and Structures, 40(22), 6189-6209. DOI: 10.1016/s0020-7683(03)00388-3
22. Jones, R. M. (2009). Deformation Theory of Plasticity. Blacksburg: Bull Ridge Corporation, 640p.
23. Zolochevsky, A. A., Sklepus, A. N., Sklepus, S. N. (2011). Nonlinear Solid Mechanics. Kharkiv: Garant, 719p. https://www.researchgate.net/publication/259973086
24. Nemat-Nasser, S., Hori, M. (1993). Micromechanics: Overall Properties of Heterogeneous Materials. Amsterdam: Elsevier, 669p.
25. Dvorak, G. (2012). Micromechanics of Composite Materials. Dordrecht: Springer, 442p. DOI: 10.1007/978-94-007-4101-0
26. Aboudi, J., Arnold, S. M., Bednarcyk, B. A. (2013). Micromechanics of Composite Materials: A Generalized Multiscale Analysis Approach. Oxford: Butterworth-Heinemann, 984p. DOI: 10.1016/C2011-0-05224-9
27. Yin, H., Zhao, Y. (2016). Introduction to the Micromechanics of Composite Materials. Boca Raton: CRC Press, 218p. DOI: 10.1201/b19685
28. Taya, M., Arsenault, R. J. (1987). A comparison between a shear lag type model and an eshelby type model in predicting the mechanical properties of a short fiber composite. Scripta Metallurgica, 21(3), 349-354.
29. Wang, Y., Huang, Z. (2018). Analytical micromechanics models for elastoplastic behavior of long fibrous composites: A critical review and comparative study. Materials, 11, 1919-1–1919-55. DOI: 10.3390/ ma11 101919
30. Mondali, M., Abedian, A., Ghavami, A. (2009). A new analytical shear-lag based model for prediction of the steady state creep deformations of some short fiber composites. Materials & Design, 30(4), 1075-1084. DOI: 10.1016/j.matdes.2008.06.039
31. Mondali, M., Monfared, V., Abedian, A. (2013). Non-linear creep modeling of short-fiber composites using Hermite polynomials, hyperbolic trigonometric functions and power series. Comptes Rendus Mecanique, 341(7), 592-604. DOI: 10.1016/j.crme.2013.04.004
32. Monfared, V. (2015). A displacement based model to determine the steady state creep strain rate of short fiber composites. Composites Science and Technology, 107, 18-28. DOI: 10.1016/j.compscitech.2014.11.019
33. Li, Y., Li, S., Li, Z. (2014). Interface diffusion-induced creep and stress relaxation in unidirectional metal matrix composites under biaxial loading. Mechanics of Materials, 76, 20-26. DOI: 10.1016/j.mechmat.2014 .05.003
34. Sun, Y., Li, A., Ren, X., Lu, Y., Liu, M. (2017). Interface diffusion-induced creep in metal matrix particulate composites under triaxial loading. Acta Mechanica, 228(7), 2471-2481. DOI: 10.1007/s00707-017-1832-5
35. Xu, B., Guo, F. (2019). A micromechanics method for transverse creep behavior induced by interface diffusion in unidirectional fiber-reinforced metal matrix composites. International Journal of Solids and Structures, 159, 126-134. DOI: 10.1016/j.ijsolstr.2018.09.024
36. Xu, B., Xu, W., Guo, F. (2020). Creep behavior due to interface diffusion in unidirectional fiber-reinforced metal matrix composites under general loading conditions: A micromechanics analysis. Acta Mechanica, 231(4), 1321-1335. DOI: 10.1007/s00707-019-02592-8
37. Fernández, R., González-Doncel, G. (2009). Load partitioning during creep of powder metallurgy metal matrix composites and shear-lag model predictions. Materials Science and Engineering A, 500(1-2), 109-113. DOI: 10.1016/j.msea.2008.09.041
38. Kanouté, P., Boso, D. P., Chaboche, J. L., Schrefler, B. (2009). Multiscale methods for composites: A review. Archives of Computational Methods in Engineering, 16(1), 31-75. DOI: 10.1007/s11831-008-9028-8
39. Wu, L., Noels, L., Adam, L., Doghri, I. (2013). A combined incremental-secant mean-field homogenization scheme with per-phase residual strains for elasto-plastic composites. International Journal of Plasticity, 51, 80-102. DOI: 10.1016/j.ijplas.2013.06.006
40. Kruch, S., Chaboche, J. L. (2011). Multi-scale analysis in elasto-viscoplasticity coupled with damage. International Journal of Plasticity, 27(12), 2026-2039. DOI: 10.1016/j.ijplas.2011.03.007
41. Yancey, R. N., Pindera, M. J. (1990). Micromechanical analysis of the creep response of unidirectional composites. Transactions of the ASME. Journal of Engineering Materials and Technology, 112,157-163. DOI:10.1115/1.2903302
42. Barral, M., Chatzigeorgiou, G., Meraghni, F., Léon, R. (2020). Homogenization using modified Mori-Tanaka and TFA framework for elastoplastic-viscoelastic-viscoplastic composites: Theory and numerical validation. International Journal of Plasticity, 127, 102632. DOI: 10.1016/j.ijplas.2019.11.011
43. Chen, Q., Chatzigeorgiou, G., Meraghni, F. (2021). Extended mean-field homogenization of viscoelastic-viscoplastic polymer composites undergoing hybrid progressive degradation induced by interface debonding and matrix ductile damage. International Journal of Solids and Structures, 210, 1-17. DOI: 10.1016/j.ijsolstr.2020.11.017
44. Cruz-González, O. L., Ramírez-Torres, A., Rodríguez-Ramos, R., Otero, J. A., Penta, R., Lebon, F. (2021). Effective behavior of long and short fiber-reinforced viscoelastic composites. Applications in Engineering Science, 6, 100037. DOI: 10.1016/j.apples.2021.100037

45. He, Z. (2022). Finite volume based asymptotic homogenization of viscoelastic unidirectional composites. Composite Structures, 291, 115601. DOI: 10.1016/j.compstruct.2022.115601
46. Chen, Q., Chatzigeorgiou, G., Robert, G., Meraghni, F. (2022). Viscoelastic-viscoplastic homogenization of short glass-fiber reinforced polyamide composites (PA66/GF) with progressive interphase and matrix damage: New developments and experimental validation. Mechanics of Materials, 164, 104081. DOI: 10.1016/j.mechmat.2021.104081
47. Lahellec, N., Suquet, P. (2007). On the effective behavior of nonlinear inelastic composites: I. Incremental variational principles. Journal of the Mechanics and Physics of Solids, 55(9), 1932-1963. DOI: 10.1016/j.jmps.2007.02.003
48. Hine, P. J., Gusev, A. A. (2019). Validating a micromechanical modelling scheme for predicting the five independent viscoelastic constants of unidirectional carbon fibre composites. International Journal of Engineering Science, 144, 103133. DOI: 10.1016/j.ijengsci.2019.103133
49. Ju, X., Mahnken, R., Xu, Y., Liang, L., Zhou, W. (2021). A nonuniform transformation field analysis for composites with strength difference effects in elastoplasticity. International Journal of Solids and Structures, 228, 111103-1–111103-16. DOI:10.1016/j.ijsolstr.2021.111103
50. Chun, H. J., Daniel, I. M. (1997). Transverse creep behavior of a unidirectional metal matrix composite. Mechanics of Materials, 25(1), 37-46. DOI: 10.1016/s0167-6636(96)00049-x
51. Tsukamoto, H. (2010). A mean-field micromechanical formulation of a nonlinear constitutive equation of a two-phase composite. Computational Materials Science, 50(2), 560-570. DOI: 10.1016/j.commatsci.2010.09.019
52. Katouzian, M., Vlase, S. (2020). Creep response of neat and carbon-fiber-reinforced PEEK and epoxy determined using a micromechanical model. Symmetry, 12(10), 1680. DOI: 10.3390/sym12101680
53. Wu, X., Ohno, N. (1999). A homogenization theory for time-dependent nonlinear composites with periodic internal structures. International Journal of Solids and Structures, 36(33), 4991-5012. DOI: 10.1016/s0020-7683(98)00236-4
54. Shojaei, A., Li, G., Fish, J., Tan, P. J. (2014). Multi-scale constitutive modeling of ceramic matrix composites by continuum damage mechanics. International Journal of Solids and Structures, 51(23-24), 4068-4081. DOI: 10.1016/j.ijsolstr.2014.07.026
55. Kumar, R. S., Mordasky, M., Ojard, G., Yuan, Z., Fish, J. (2019). Notch-strength prediction of ceramic matrix composites using multi-scale continuum damage model. Materialia, 6, 100267. DOI:10.1016/j.mtla.2019.100267
56. Artz, T., Yuan, Z., Kumar, R., Fish, J. (2020). Computational model for oxidation-assisted rupture of ceramic matrix composites. International Journal of Solids and Structures, 202, 195-207. DOI: 10.1016/j.ijsolstr.2020.05.009
57. Artz, T., Fish, J. (2021). A unified approach to computational modeling of ceramic matrix composites under high-temperature creep, fatigue, and initial quasi-static loading. International Journal for Multiscale Computational Engineering, 19(5), 61-99. DOI: 10.1615/IntJMultCompEng.2021040894
58. Khafagy, K. H., Sorini, C., Skinner, T., Chattopadhyay, A. (2021). Modeling creep behavior in ceramic matrix composites. Ceramics International, 47(9), 12651–12660. DOI: 10.1016/j.ceramint.2021.01.125
59. Xu, H., Kuczynska, M., Schafet, N., Welschinger, F., Hohe, J. (2022). FE-based damage modeling approach for short fiber reinforced thermoplastics under quasi-static load coupling anisotropic viscoplasticity and matrix degradation. Journal of Composite Materials, 56(20), 3113-3125. DOI: 10.1177/00219983221109327
60. Brinson, L. C., Lin, W. S. (1998). Comparison of micromechanics methods for effective properties of multiphase viscoelastic composites. Composite Structures, 41(3-4), 353-367. DOI: 10.1016/S0263-8223(98)00019-1
61. Fisher, F. T., Brinson, L. C. (2001). Viscoelastic interphases in polymer–matrix composites: Theoretical models and finite-element analysis. Composites Science and Technology, 61(5), 731-748. DOI: 10.1016/S0266-3538(01)00002-1
62. Allen, D. H., Jones, R. H., Boyd, J. G. (1994). Micromechanical analysis of a continuous fiber metal matrix composite including the effects of matrix viscoplasticity and evolving damage. Journal of the Mechanics and Physics of Solids, 42(3), 505-529. DOI: 10.1016/0022-5096(94)90029-9
63. Feyel, F., Chaboche, J. L. (2000). FE^2 multiscale approach for modelling the elastoviscoplastic behaviour of long fibre SiC/Ti composite materials. Computer Methods in Applied Mechanics and Engineering, 183(3-4), 309-330. DOI: 10.1016/s0045-7825(99)00224-8
64. Niordson, C. F., Tvergaard, V. (2001). Nonlocal plasticity effects on the tensile properties of a metal matrix composite. European Journal of Mechanics-A/Solids, 20(4), 601-613. DOI: 10.1016/S0997-7538(01)01149-4
65. Bonora, N., Ruggiero, A. (2006). Micromechanical modeling of composites with mechanical interface–Part 1: Unit cell model development and manufacturing process effects. Composites Science and Technology, 66(2), 314-322. DOI: 10.1016/j.compscitech.2005.04.041

66. Bonora, N., Ruggiero, A. (2006). Micromechanical modeling of composites with mechanical interface–Part II: Damage mechanics assessment. Composites Science and Technology, 66(2), 323-332. DOI: 10.1016/j.compscitech.2005.04.043
67. Aghdam, M. M., Falahatgar, S. R. (2004). Micromechanical modeling of interface damage of metal matrix composites subjected to transverse loading. Composite Structures, 66(1-4), 415-420. DOI: 10.1016/j.compstruct.2004.04.063
68. Aghdam, M. M., Falahatgar, S. R., Gorji, M. (2008). Micromechanical consideration of interface damage in fiber reinforced Ti-alloy under various combined loading conditions. Composites Science and Technology, 68(15-16), 3406-3411. DOI: 10.1016/j.compscitech.2008.09.028
69. Mahmoodi, M. J., Aghdam, M. M., Shakeri, M. (2010). Micromechanical modeling of interface damage of metal matrix composites subjected to off-axis loading. Materials & Design, 31(2), 829-836. DOI: 10.1016/j.matdes.2009.07.048
70. Lüders, C. (2020). Nonlinear-elastic orthotropic material modeling of an epoxy-based polymer for predicting the material behavior of transversely loaded fiber-reinforced composites. Journal of Composites Science, 4(2), 46. DOI: 10.3390/jcs4020046
71. Faucon, A., Martin, E., Coutand, B., Carrere, N., Fromentin, J. F., Molliex, L., Dambrine, B. (2002). Longitudinal creep behaviour of a SiC/Ti-6242 composite in a vacuum atmosphere. Applied Composite Materials, 9(6), 379-393. DOI: 10.1023/a:1020214908942
72. Martin, E., CarrÉre, N. (2011). Metal matrix composites: Continuous silicon-carbide fibers/titanium-alloy matrix. In Nicolais, L. and Borzacchiello, A. (eds.), Wiley Encyclopedia of Composites (pp. 1695- 1706), Vol. 3, Second Edition. New York: John Wiley & Sons. DOI: 10.1002/9781118097298.weoc139
73. Ahmadi, I., Ataee, N. (2016). Micromechanical modeling for prediction of the creep behavior of fibrous composite materials. Modares Mechanical Engineering, 16(8), 249-260. https://mme.modares.ac.ir/files/mme/user_files_749497/archive_global-A-15-1000-607-e520207.pdf
74. Fliegener, S., Hohe, J. (2020). An anisotropic creep model for continuously and discontinuously fiber reinforced thermoplastics. Composites Science and Technology, 194, 108168. DOI:10.1002/pamm.201900086
75. Wang, Z., Smith, D. E. (2019). Numerical analysis on viscoelastic creep responses of aligned short fiber reinforced composites. Composite Structures, 229, 111394. DOI: 10.1016/j.compstruct.2019.111394
76. Liu, Y., Van der Meer, F. P., Sluys, L. J., Fan, J. T. (2020). A numerical homogenization scheme used for derivation of a homogenized viscoelastic-viscoplastic model for the transverse response of fiber-reinforced polymer composites. Composite Structures, 252, 112690. DOI: 10.1016/j.compstruct.2020.112690
77. Katouzian, M., Vlase, S., Scutaru, M. L. (2021). Finite Element Method-Based Simulation Creep Behavior of Viscoelastic Carbon-Fiber Composite. Polymers, 13(7), 1017. DOI: 10.3390/polym 13071017
78. Drosopoulos, G. A., Stavroulakis, G. E. (2022). Nonlinear Mechanics for Composite Heterogeneous Structures. Boca Raton: CRC Press, 284p. DOI: 10.1201/9781003017240
79. Hayat, M. D., Singh, H., He, Z., Cao, P. (2019). Titanium metal matrix composites: An overview. Composites Part A: Applied Science and Manufacturing, 121, 418-438. DOI: 10.1016/j.compositesa.2019.04.00
80. Bettge, D., Günther, B., Wedell, W., Portella, P. D., Hemptenmacher, J., Peters, P. W., Skrotzki, B. (2007). Mechanical behavior and fatigue damage of a titanium matrix composite reinforced with continuous SiC fibers. Materials Science and Engineering: A, 452, 536-544. DOI: 10.1016/j.msea.2006.10.107
81. Peters, P. W. M., Hemptenmacher, J., Günther, B., Bettge, D., Portella, P. (2004). Analysis of the thermo-mechanical fatigue behaviour of SiC-fibre reinforced titanium alloy (SCS-6/TI-6242). In From Nano-Scale Interactions to Engineering Structures: 11th European Conference on Composite Materials (May 31–June 3, 2004, Rhodos, Vol. 2, pp. 1-8). Rhodos: ESCM. http://www.escm.eu.org/docs/eccm/C158.pdf
82. Metal matrix composites. (2002). In Military Handbook - MIL-HDBK-17-4A: Composite Materials Handbook, Vol. 4. Washington: U.S. Department of Defense, 168p. https://www.library.ucdavis.edu/wp-content/uploads/2017/03/HDBK17-4A.pdf
83. Withers, P. J., Bennett, J. A., Kuroda, M. (2010). Interfacial shear strength behaviour of Ti/SiC metal matrix composites at room and elevated temperature. Acta Materialia, 58(18), 6090-6103. DOI: 10.1016/j.actamat.2010.07.027
84. Carrere, N., Martin, E., Coutand, B. (2003). Creep behaviour of a unidirectional SM1140+/Ti-6242 composite. Composites Part A: Applied Science and Manufacturing, 34(11), 1065-1073. DOI: 10.1016/S1359-835X(03)00212-4
85. Carrère, N., Kruch, S., Vassel, A., Chaboche, J. L. (2002). Damage mechanisms in unidirectional SiC/Ti composites under transverse creep loading: Experiments and modeling. International Journal of Damage Mechanics, 11(1), 41-63. DOI: 10.1106/105678902022261
86. Nikitenko, A. F., Sosnin, O. V., Torshenov, N. G., Shokalo, I. K. (1971). Creep of hardening materials with different properties in tension and compression. Journal of Applied Mechanics and Technical Physics, 12(2), 277-281. DOI: 10.1007/BF00850702

87. Nikitenko, A. F., Sosnin, O. V., Torshenov, N. G., Shokalo, I. K. (1976). Strength characteristics of titanium alloys. Journal of Applied Mechanics and Technical Physics, 17(6), 849-852. DOI: 10.1007/BF00858112
88. Deka, D., Joseph, D. S., Ghosh, S., Mills, M. J. (2006). Crystal plasticity modeling of deformation and creep in polycrystalline Ti-6242. Metallurgical and Materials Transactions A, 37(5), 1371-1388. DOI: 10.1007/s11661-006-0082-2
89. Zolochevskii, A. A. (1986). Verification of the governing equations for the nonlinear deformation of materials with different strengths in tension and compression. Journal of Applied Mechanics and Technical Physics, 27(6), 913-917. DOI: 10.1007/bf00918838
90. Zolochevskii, A. A. (1988). Modification of the theory of plasticity of materials differently resistant to tension and compression for simple loading processes. Soviet Applied Mechanics, 24(12), 1212-1217. DOI: 10.1007/bf00887929
91. Zolochevskii, A. A. (1990). Method of calculating the strength of mine pipes formed from materials that behave differently under tension and compression. Strength of Materials, 22(3), 422-428. DOI: 10.1007/BF00768204
92. Zolochevskii, A. A. (1990). Determining equations of nonlinear deformation with three stress-state invariants. Soviet Applied Mechanics, 26(3), 277-282. DOI: 10.1007/BF00937216
93. Altenbach, H., Krause, J., Zolochevsky, A. (1992). Herleitung von Konstitutivgleichungen für Werkstoffe mit komplizierten Eigenschaften. Zeitschrift für angewandte Mathematik und Mechanik, 72(4), T181-T183. DOI: 10.1002/zamm.19920720405h
94. Zolochevskii, A. A., Koz'min, Y. S. (1993). Nonlinear deformation of rectangular thick-walled shells consisting of material that responds differently to tension and compression. International Applied Mechanics, 29(8), 624-630. DOI: 10.1007/BF00847012
95. Zolochevskii, A. A. (1993). Nonlinear asymmetric deformation of composite shells formed from materials having different tensile and compressive strengths. International Applied Mechanics, 29(11), 945-951. DOI: 10.1007/BF00848280
96. Mahnken, R., Schlimmer, M. (2005). Simulation of strength difference in elasto-plasticity for adhesive materials. International journal for numerical methods in engineering, 63(10), 1461-1477.
97. Zolochevsky, A., Yeseleva, E., Ehlers, W. (2005). An anisotropic model of damage for brittle materials with different behavior in tension and compression. Forschung im Ingenieurwesen, 69(3), 170-180. DOI: 10.1007/s10010-005-0150-6
98. Hu, W., Wang, Z. R. (2005). Multiple-factor dependence of the yielding behavior to isotropic ductile materials. Computational Materials Science, 32(1), 31-46. DOI: 10.1016/j.commatsci.2004.06.002
99. Hashiguchi, K., Mase, T. (2007). Extended yield condition of soils with tensile yield strength and rotational hardening. International Journal of Plasticity, 23(12), 1939-1956. DOI: 10.1016/j.ijplas.2007.07.011
100. Öchsner, A., Mishuris, G. (2009). Modelling of the multiaxial elasto-plastic behaviour of porous metals with internal gas pressure. Finite Elements in Analysis and Design, 45(2), 104-112. DOI: 10.1016/j.finel.2008.07.007
101. Madhi, E., Nagy, P. B. (2011). Sensitivity analysis of a directional potential drop sensor for creep monitoring. NDT & E International, 44(8), 708-717. DOI: 10.1016/j.ndteint.2011.08.001
102. Lanoye, E., Dormieux, L., Kondo, D. (2014). A micromechanical-based damage analysis of a cylindrical bar under torsion: Theoretical results, finite elements verification and application. Theoretical and Applied Fracture Mechanics, 74, 116-125. DOI: 10.1016/j.tafmec.2014.08.006
103. Zolochevsky, O. O., Martynenko, O. V. (2019). Biomechanical analysis of tension-compression asymmetry, anisotropy and heterogeneity of bone reconstruction in response to periprosthetic fracture repair. The Journal of V. N. Karazin Kharkiv National University: Medicine, (37), 19-32. DOI: 10.26565/2313-6693-2019-37-03
104. Zhang, Y., Jar, P-Y. B., Xue, S., Li, L. (2019). Numerical simulation of ductile fracture in polyethylene pipe with continuum damage mechanics and Gurson-Tvergaard-Needleman damage models. Proceedings of the Institution of Mechanical Engineers, Part L: Journal of Materials: Design and Applications, 233(12), 2455-2468. DOI: 10.1177/1464420719863458
105. Zolochevsky, A., Martynenko, A. (2020). Neuromechanical characterization of brain damage in response to head impact and pathological changes. The Journal of V. N. Karazin Kharkiv National University: Medicine, (39), 5-25. DOI: 10.26565/2313-6693-2020-39-01
106. Drass, M. (2020). Constitutive Modelling and Failure Prediction for Silicone Adhesives in Façade Design. Wiesbaden: Springer, 291p. DOI: 10.1007/978-3-658-29255-3
107. Maghous, S., de Aguiar, C. B., Rossi, R. (2021). Micromechanical approach to effective viscoelastic behavior of jointed rocks. International Journal of Rock Mechanics and Mining Sciences, 139, 104581. DOI: 10.1016/j.ijrmms.2020.104581
108. Zhang, L., Lu, M., Han, L., Cao, J. (2021). A model reduction method for nonlinear analysis of materials and structures with tension–compression asymmetric properties. Composite Structures, 262, 113613-1–113613-13. DOI: 10.1016/j. compstruct.2021.113613

109. Zolochevsky, O. O., Parkhomenko, S. S., Martynenko, O. V. (2022). Quantum, molecular and continuum modeling in nonlinear mechanics of viruses. The Journal of V. N. Karazin Kharkiv National University: Medicine, (44), 5-34. DOI: 10.26565/2313-6693-2022-44-01
110. Zolochevsky, A. A. (1980). Allowance for differences in tension and compression for materials in the creep problems of shells. Dynamics and Strength of Machines, (32), 8–13. https://www.researchgate.net/publication/259757353
111. Zolochevsky, A. A. (1982). Creep of Thin Shells for Materials with Different Behavior in Tension and Compression. Ph. D. Thesis, Kharkiv: National Academy of Sciences of Ukraine, Institute of Mechanical Engineering Problems, 198p. DOI: 10.13140/RG.2.2.21795.20000
112. Zolochevskii, A. A. (1988). Effect of the type of loading on the creep of isotropic strain-hardening materials. Soviet Applied Mechanics, 24(2), 185-191. DOI: 10.1007/bf00883831
113. Zolochevskij, A. A. (1988). Kriechen von Konstruktionselementen aus Materialien mit von der Belastung abhängigen Charakteristiken. Technische Mechanik, 9(3), 177-184. https://www.researchgate.net/publication/351991514
114. Altenbach, H., Zolochevsky, A. (1991). Kriechen dünner Schalen aus anisotropen Werkstoffen mit unterschiedlichem Zug-Druck-Verhalten. Forschung im Ingenieurwesen, 57(6), 172-179. DOI:10.1007/BF02575157
115. Altenbach, H., Schieße, P., Zolochevsky, A. A. (1991). Zum Kriechen isotroper Werkstoffe mit komplizierten Eigenschaften. Rheologica acta, 30(4), 388-399. DOI: 10.1007/BF00404197
116. Altenbach, H., Zolochevsky, A. A. (1994). Eine energetische Variante der Theorie des Kriechens und der Langzeitfestigkeit für isotrope Werkstoffe mit komplizierten Eigenschaften. Zeitschrift für Angewandte Mathematik und Mechanik, 74(3), 189-199. DOI: 10.1002/zamm.19940740311
117. Betten, J., Sklepus, A., Zolochevsky, A. (2003). A constitutive theory for creep behavior of initially isotropic materials sustaining unilateral damage. Mechanics Research Communications, 30(3), 251-256. DOI: 10.1016/s0093-6413(03)00002-8
118. Zolochevsky, A., Galishin, A., Kühhorn, A., Springmann, M. (2009). Transversal shear effect in moderately thick shells from materials with characteristics dependent on the kind of stress state under creep-damage conditions: Theoretical framework. Technische Mechanik, 29(1), 38-47. https://www.researchgate.net/publication/259973257
119. Galishin, A., Zolochevsky, A., Kühhorn, A., Springmann, M. (2009). Transversal shear effect in moderately thick shells from materials with characteristics dependent on the kind of stress state under creep-damage conditions: Numerical modeling. Technische Mechanik, 29(1), 48-59. https://www.researchgate.net/publication/228517955
120. Zolochevsky, A., Hop, J. G., Servant, G., Foosnæs, T., Øye, H. A. (2003). Creep and sodium expansion in a semigraphitic cathode carbon. In Crepeau P. N. (ed.), Light Metals (pp. 595-602). Warrendale: The Minerals, Metals and Materials Society. https://www.researchgate.net/publication/263891462
121. Challamel, N., Lanos, C., Casandjian, C. (2005). Creep damage modelling for quasi-brittle materials. European Journal of Mechanics-A/Solids, 24(4), 593-613. DOI: 10.1016/j.euromechsol.2005.05.003
122. Mahnken, R. (2005). Creep simulation of asymmetric effects at large strains by stress mode decomposition. Computer methods in applied mechanics and engineering, 194(39-41), 4221-4243. DOI: 10.1016/j.cma.2004.11.003
123. Zolochevsky, A., Hop, J. G., Foosnæs, T., Øye, H. A. (2005). Surface exchange of sodium, anisotropy of diffusion and diffusional creep in carbon cathode materials. In Kvande H. (ed.), Light Metals (pp. 745-750). San Francisco: The Minerals, Metals and Materials Society. https://www.researchgate.net/publication/263891523
124. Artzt, K., Hackemann, S., Flucht, F., Bartsch, M. (2015). Anisotropic creep behavior of a unidirectional all-oxide CMC. In Singh D. and Salem J. (eds.), Mechanical Properties and Performance of Engineering Ceramics and Composites IX (pp.). Hoboken: Wiley. DOI: 10.1002/9781119031192.ch1
125. Liu, Y. R., Zhang, L., Yang, Q. (2015). A creep damage model for rock mass based on internal variable theory. Applied Mechanics and Materials, 784, 19-26. DOI: 10.4028/www.scientific.net/AMM.784.19
126. Zhang, Q., Zhang, W., Liu, Y. (2015). Evaluation and mathematical modeling of asymmetric tensile and compressive creep in aluminum alloy ZL109. Materials Science and Engineering: A, 628, 340-349. DOI: 10.1016/j.msea.2015.01.032
127. Dusserre, G., Valentin, O., Nazaret, F., Cutard, T. (2016). Experimental and numerical investigation of the asymmetric primary creep of a fibre reinforced refractory concrete at 1200° C. Journal of the European Ceramic Society, 36(10), 2627-2639. DOI: 10.1016/j.jeurceramsoc.2016.03.007
128. Chowdhury, H., Naumenko, K., Altenbach, H., Krüger, M. (2017). Rate dependent tension-compression-asymmetry of Ti-61.8 at% Al alloy with long period superstructures at 1050 C. Materials Science and Engineering: A, 700, 503-511. DOI: 10.1016/j.msea.2017.06.041
129. Jiménez, S., Duddu, R., Bassis, J. (2017). An updated-Lagrangian damage mechanics formulation for

modeling the creeping flow and fracture of ice sheets. Computer Methods in Applied Mechanics and Engineering, 313, 406-432. DOI: 10.1016/j.cma.2016.09.034

130. Li, Y., Shi, Z., Lin, J., Yang, Y. L., Rong, Q., Huang, B. M., Chung, T. F., Tsao, C. S., Yang, J. R., Balint, D. S. (2017). A unified constitutive model for asymmetric tension and compression creep-ageing behaviour of naturally aged Al-Cu-Li alloy. International Journal of Plasticity, 89, 130-149. DOI: 10.1016/j.ijplas.2016.11.007
131. Li, Y., Shi, Z., Lin, J., Yang, Y. L., Saillard, P., Said, R. (2018). FE simulation of asymmetric creep-ageing behaviour of AA2050 and its application to creep age forming. International Journal of Mechanical Sciences, 140, 228-240. DOI: 10.1016/j.ijmecsci.2018.03.003
132. Li, L., Guan, J., Xiao, M., Zhuo, L. (2021). Three-dimensional creep constitutive model of transversely isotropic rock. International Journal of Geomechanics, 21(8), 04021124. DOI: 10.1061/(ASCE)GM.1943-5622.0002111
133. Yang, Y., Zhan, L., Liu, C., Xu, Y., Li, G., Wu, X., Huang, M., Hu, Z. (2021). Tension-compression asymmetry of stress-relaxation ageing behavior of AA2219 alloy over a wide range of stress levels. Materials Science and Engineering: A, 823, 141730. DOI: 10.1016/j.msea.2021.141730
134. Huth, A., Duddu, R., Smith, B. (2021). A generalized interpolation material point method for shallow ice shelves. 2: Anisotropic nonlocal damage mechanics and rift propagation. Journal of Advances in Modeling Earth Systems, 13, e2020MS002292-1– e2020MS002292-26. DOI: 10.1029/2020MS002292
135. Jin, S., Harmuth, H. (2021). Asymmetric creep modeling of common refractory ceramics with high temperature wedge splitting test. Engineering Fracture Mechanics, 252, 107819-1-107819-12. DOI:10.1016/j.engfracmech.2021. 107819
136. Zolochevskyi, O. O., Parkhomenko, L. O., Martynenko, O. V. (2021). Effect of non-stoichiometry and difference between the tensile and compressive moduli of elasticity of perovskite on the diffusion creep of a thick-walled perovskite cylinder. International Applied Mechanics, 57(3), 336-346. https://www.researchg ate.net/publication/359991604
137. Zolochevsky, A., Parkhomenko, S. (2022). Diffusion creep analysis in perovskite thick-walled cylinder under radial oxygen vacancies gradient. Structural Integrity and Life, 22(1), 57-62. https://www.researchgate.net /publication/358898949
138. Guo, Y., Liu, G., Huang, Y. (2022). A complemented multiaxial creep constitutive model for materials with different properties in tension and compression. European Journal of Mechanics-A/Solids, 93, 104510. DOI: 10.1016/j.euromechsol.2022.104510
139. Mao, X., Zhang, J., Yuan, P., Yan, F., Wang, H., Jian, X., Lu, C., Ding, S., Li, Y. (2022). An innovative multi-layer shell model for in-pile thermo-mechanical behavior analysis of plate-type fuel assemblies. Composite Structures, 293, 115735. DOI: 10.1016/j.compstruct.2022.115735
140. Coules, H. E., Nneji, S. O., James, J. A., Kabra, S., Hu, J. N., Wang, Y. (2022). Full-tensor measurement of multiaxial creep stress relaxation in type 316H stainless steel. Experimental Mechanics, 62(1), 19-33. DOI: 10.1007/s11340-021-00755-0
141. Neeraj, T., Savage, M. F., Tatalovich, J., Kovarik, L., Hayes, R. W., Mills, M. J. (2005). Observation of tension–compression asymmetry in α and α/β titanium alloys. Philosophical Magazine, 85(2-3), 279-295. DOI: 10.1080/14786430412331315707
142. Chrzan, D. C. (2021). Asymmetry in deformation. Nature Materials, 20(10), 1305-1306. DOI: 10.1038/s41563-021-01107-y
143. Greenwood, G. W. (1992). A formulation for anisotropy in diffusional creep. Proceedings of the Royal Society of London. Series A: Mathematical and Physical Sciences, 436(1896), 187-196. DOI: 10.2307/52028
144. Svoboda, J., Lukáš, P. (2000). Creep deformation modelling of superalloy single crystals. Acta Materialia, 48(10), 2519-2528. DOI: 10.1016/S1359-6454(00)00078-1
145. Naumenko, K., Altenbach, H. (2005). A phenomenological model for anisotropic creep in a multipass weld metal. Archive of Applied Mechanics, 74(11), 808-819. DOI: 10.1007/s00419-005-0409-2
146. Peravali, S., Hyde, T. H., Cliffe, K. A., Leen, S. B. (2009). An anisotropic creep damage model for anisotropic weld metal. Transactions of the ASME. Journal of Pressure Vessel Technology, 131(2). DOI: 10.1115/1.3007429
147. Vladimirov, I. N., Reese, S., Eggeler, G. (2009). Constitutive modelling of the anisotropic creep behaviour of nickel-base single crystal superalloys. International Journal of Mechanical Sciences, 51(4), 305-313. DOI: 10.1016/j.ijmecsci.2009.02.004
148. Stewart, C. M., Gordon, A. P., Ma, Y. W., Neu, R. W. (2011). An anisotropic tertiary creep damage constitutive model for anisotropic materials. International Journal of Pressure Vessels and Piping, 88(8-9), 356-364. DOI: 10.1016/j.ijpvp.2011.06.010
149. Shi, D., Dong, C., Yang, X. (2013). Constitutive modeling and failure mechanisms of anisotropic tensile and creep behaviors of nickel-base directionally solidified superalloy. Materials & Design, 45, 663-673. DOI: 10.1016/j.matdes.2012.09.031

150. Martin, G., Ochoa, N., Sai, K., Hervé-Luanco, E., Cailletaud, G. (2014). A multiscale model for the elastoviscoplastic behavior of directionally solidified alloys: Application to FE structural computations. International Journal of Solids and Structures, 51(5), 1175-1187. DOI: 10.1016/j.ijsolstr.2013.12.013
151. Trinh, B. T., Hackl, K. (2014). A model for high temperature creep of single crystal superalloys based on nonlocal damage and viscoplastic material behavior. Continuum Mechanics and Thermodynamics, 26(4), 551-562. DOI: 10.1007/s00161-013-0317-6
152. Wen, Z., Zhang, D., Li, S., Yue, Z., Gao, J. (2017). Anisotropic creep damage and fracture mechanism of nickel-base single crystal superalloy under multiaxial stress. Journal of Alloys and Compounds, 692, 301-312. DOI: 10.1016/j.jallcom.2016.09.052
153. Cao, L., Wollgramm, P., Bürger, D., Kostka, A., Cailletaud, G., Eggeler, G. (2018). How evolving multiaxial stress states affect the kinetics of rafting during creep of single crystal Ni-base superalloys. Acta Materialia, 158, 381-392. DOI: 10.1016/j.actamat.2018.07.061
154. Naumenko, K., Gariboldi, E. (2022). Experimental analysis and constitutive modeling of anisotropic creep damage in a wrought age-hardenable Al alloy. Engineering Fracture Mechanics, 259, 108119. DOI: 10.1016/j.engfracmech.2021.108119
155. Chen, L., Liu, C., Ma, P., Yang, J., Zhan, L., Huang, M. (2022). Strong in-plane anisotropy of creep ageing behavior in largely pre-deformed Al-Cu alloy: Experiments and constitutive modeling. International Journal of Plasticity, 152, 103245. DOI: 10.1016/j.ijplas.2022.103245
156. Hausmann, J. M., Leyens, C., Kaysser, W. A. (2004). Interaction between cyclic loading and residual stresses in titanium matrix composites. Journal of Materials Science, 39(2), 501-509. DOI: 10.1023/B:JMSC.0000011505.78250.ad
157. Bourbita, F., Rémy, L., Köster, A. (2009). Thermal-mechanical fatigue behaviour of a titanium matrix composite reinforced with long SiC fibers. In Proceedings of the 17th International Conference on Composite Materials (27-31 July 2009, Edinburgh, United Kingdom). London: IOM Communications Ltd, 10p. http://iccm-central.org/Proceedings/ICCM17proceedings/papers/D8.14%20Bourbita.pdf
158. Feng, G. H., Yang, Y. Q., Luo, X., Li, J., Huang, B., Chen, Y. (2015). Fatigue properties and fracture analysis of a SiC fiber-reinforced titanium matrix composite. Composites Part B: Engineering, 68, 336-342. DOI: 10.1016/j.compositesb.2014.09.005
159. Bathias, C., Paris, P. C. (2004). Gigacycle Fatigue in Mechanical Practice. New York: CRC Press, 328 p. DOI: 10.1201/9780203020609
160. Brommesson, R., Hörnqvist, M., Ekh, M. (2014). Low-cycle fatigue crack growth in Ti-6242 at elevated temperature. Advanced Materials Research, 891-892, 422-427. DOI: 10.4028/www.scientific.net/AMR.891-892.422
161. Heckel, T. K., Christ, H. J. (2010). Isothermal and thermomechanical fatigue of titanium alloys. Procedia Engineering, 2(1), 845-854. DOI: 10.1016/j.proeng.2010.03.091
162. Barriobero-Vila, P., Requena, G., Warchomicka, F., Stark, A., Schell, N., Buslaps, T. (2015). Phase transformation kinetics during continuous heating of a β-quenched Ti–10V–2Fe–3Al alloy. Journal of Materials Science, 50(3), 1412-1426. DOI: 10.1007/s10853-014-8701-6
163. Barriobero-Vila, P., Requena, G., Schwarz, S., Warchomicka, F., Buslaps, T. (2015). Influence of phase transformation kinetics on the formation of α in a β-quenched Ti–5Al–5Mo–5V–3Cr–1Zr alloy. Acta Materialia, 95, 90-101. DOI: 10.1016/j.actamat.2015.05.008
164. Kassner, M. E., Kosaka, Y., Hall, J. S. (1999). Low-cycle dwell-time fatigue in Ti-6242. Metallurgical and Materials Transactions A, 30(9), 2383-2389. DOI: 10.1007/s11661-999-0246-y
165. Peters, P. W. M., Hemptenmacher, J. (2002). Oxidation of the carbon protective coating in SCS-6 fibre reinforced titanium alloys. Composites Part A: Applied Science and Manufacturing, 33(10), 1373-1379. DOI: 10.1016/S1359-835X(02)00151-3
166. Schwenker, S. W., Eylon, D. (1996). Creep deformation and damage in a continuous fiber-reinforced Ti-6Al-4V composite. Metallurgical and Materials Transactions A, 27(12), 4193-4204. DOI: 10.1007/BF02595667
167. Washizu, K. (1975). Variational Methods in Elasticity and Plasticity. Third edition, Oxford: Pergamon Press.
168. Kachanov, L. (1986). Introduction to Continuum Damage Mechanics. Dordrecht: Springer, 135p. DOI: 10.1007/978-94-017-1957-5
169. Rabotnov, Y. N. (1988). Solid Mechanics. Second Edition. Moscow: Nauka, 712p.
170. Winter, W., Heckmann, S. M., Weber, H. P. (2004). A time-dependent healing function for immediate loaded implants. Journal of Biomechanics, 37(12), 1861-1867. DOI: 10.1016/j.jbiomech.2004.02.033
171. Barbero, E. J., Greco, F., Lonetti, P. (2005). Continuum damage-healing mechanics with application to self-healing composites. International Journal of Damage Mechanics, 14(1), 51-81. DOI: 10.1177/1056789505045928
172. Darabi, M. K., Al-Rub, R. K. A., Little, D. N. (2012). A continuum damage mechanics framework for modeling micro-damage healing. International Journal of Solids and Structures, 49(3-4), 492-513. DOI:

10.1016/j.ijsolstr.2011.10.017
173. Voyiadjis, G. Z., Oucif, C., Kattan, P. I., Rabczuk, T. (2020). Damage and healing mechanics in plane stress, plane strain, and isotropic elasticity. International Journal of Damage Mechanics, 29(8), 1246-1270. DOI: 10.1177/1056789520905347
174. Zolochevsky, A., Martynenko, A., Kühhorn, A. (2012). Structural benchmark creep and creep damage testing for finite element analysis with material tension–compression asymmetry and symmetry. Computers and Structures 100-101, 27-38. DOI: 10.1016/j.compstruc.2012.02.021
175. Voyiadjis, G. Z., Thiagarajan, G. (1995). An anisotropic yield surface model for directionally reinforced metal-matrix composites. International Journal of Plasticity, 11(8), 867-894. DOI: 10.1016/S07496419(95)00 035-6
176. Voyiadjis, G. Z., Zolochevsky, A. (1998). Modeling of secondary creep behavior for anisotropic materials with different properties in tension and compression. International Journal of Plasticity, 14(10-11), 1059-1083. DOI: 10.1016/S0749-6419(98)00045-X
177. Hill, R. (1948). A theory of the yielding and plastic flow of anisotropic metals. Proceedings of the Royal Society of London. Series A. Mathematical and Physical Sciences, 193(1033), 281-297. DOI: 10.1098/rspa.1948.0045
178. Pahr, D. H., Reisinger, A. G. (2020). A review on recent advances in the constitutive modeling of bone tissue. Current Osteoporosis Reports, 18, 696-704. DOI: 10.1007/s11914-020-00631-1
179. Pasynok, M. A. (2000). Development of Anisotropic Creep Analysis Methods Taking into Account Damage of Flat Structural Elements of Machines. Ph.D Thesis, Kharkiv: National Technical University "Kharkiv Polytechnic Institute", 193p.
180. Lvov, I.G., Morachkovsky, O.K. (2009). Anisotropic creep of plates from composite materials under transverse loading. Journal of the National Technical University "Kharkiv Polytechnic Institute". Series «Dynamics and Strength of Machines», (42), 81-89.
181. Rybakina, O. G. (1982). Yield criterion for anisotropic material with SD effect, Vestnik Leningrad University, (14), 132-142.
182. Grekov, M. A. (1984). Plasticity of an anisotropic body. Doklady Akademii Nauk SSSR, 278(5), 1082–1085.
183. Efimov, I.V. (2011). Mathematical model of the yield contour for anisotropic materials. Vestnik St. Petersburg University: Mathematics, 44(1), 38-43.
184. Pavilaynen, G. V., Franus, D. V. (2021). SD-effect for circular plates of lamina cribrosa and optic nerve. Journal of Physics: Conference Series, 1959, 012035. DOI: 10.1088/1742-6596/1959/1/012035
185. Kawai, M., Zhang, J. Q., Xiao, Y., Hatta, H. (2010). Modeling of tension-compression asymmetry in off-axis nonlinear rate-dependent behavior of unidirectional carbon/epoxy composites. Journal of Composite Materials, 44(1), 75-94. DOI: 10.1177/0021998309345302
186. Kawai, M. (2011). Constitutive modeling of viscoplastic deformation of polymer matrix composites. In Guedes R.M. (ed.), Creep and Fatigue in Polymer Matrix Composites (pp. 234-272). Oxford: Woodhead Publishing. DOI: 10.1533/9780857090430.1.234
187. Kim, J. H., Lee, M. G., Chung, K., Youn, J. R., Kang, T. J. (2006). Anisotropic-asymmetric yield criterion and anisotropic hardening law for composite materials: Theory and formulations. Fibers and Polymers, 7(1), 42-50. DOI: 10.1007/BF02933601
188. Kim, J. H., Lee, M. G., Ryou, H., Chung, K., Youn, J. R., Kang, T. J. (2008). Development of nonlinear constitutive laws for anisotropic and asymmetric fiber reinforced composites. Polymer Composites, 29(2), 216-228. DOI: 10.1002/pc.20413
189. Lee, M. G., Wagoner, R. H., Lee, J. K., Chung, K., Kim, H. Y. (2008). Constitutive modeling for anisotropic/asymmetric hardening behavior of magnesium alloy sheets. International Journal of Plasticity, 24(4), 545-582. DOI: 10.1016/j.ijplas.2007.05.004
190. Wang, J., Xiao, Y. (2017). Some improvements on Sun–Chen's one-parameter plasticity model for fibrous composites. Part I: Constitutive modelling for tension–compression asymmetry response. Journal of Composite Materials, 51(3), 405-418. DOI: 10.1177/0021998316644853
191. Wang, J., Xiao, Y., Inoue, K., Kawai, M., Xue, Y. (2019). Modeling of nonlinear response in loading-unloading tests for fibrous composites under tension and compression. Composite Structures, 207, 894-908. DOI: 10.1016/j.compstruct.2018.09.054
192. Xie, Y., Xiao, Y., Lv, J., Zhang, Z., Zhou, Y., Xue, Y. (2020). Influence of creep on preload relaxation of bolted composite joints: Modeling and numerical simulation. Composite Structures, 245, 112332. DOI:10.1016/j.compstruct.2020.112332
193. Hou, Y., Min, J., Guo, N., Shen, Y., Lin, J. (2021). Evolving asymmetric yield surfaces of quenching and partitioning steels: Characterization and modeling. Journal of Materials Processing Technology, 290, 116979. DOI:10.1016/j.jmatprotec.2020.116979
194. Schwiedrzik, J. J., Wolfram, U., Zysset, P. K. (2013). A generalized anisotropic quadric yield criterion and its application to bone tissue at multiple length scales. Biomechanics and Modeling in Mechanobiology, 12(6),

1155-1168. DOI:10.1007/s10237-013-0472-5
195. Panyasantisuk, J., Pahr, D. H., Zysset, P. K. (2016). Effect of boundary conditions on yield properties of human femoral trabecular bone. Biomechanics and Modeling in Mechanobiology, 15(5), 1043-1053. DOI: 10.1007/s10237-015-0741-6
196. Schwiedrzik, J., Raghavan, R., Rüggeberg, M., Hansen, S., Wehrs, J., Adusumalli, R. B., Zimmermann, T., Michler, J. (2016). Identification of polymer matrix yield stress in the wood cell wall based on micropillar compression and micromechanical modelling. Philosophical Magazine, 96(32-34), 3461-3478. DOI: 10.1080/14786435.2016.1235292
197. Speed, A., Groetsch, A., Schwiedrzik, J. J., Wolfram, U. (2019). Extrafibrillar matrix yield stress and failure envelopes for mineralised collagen fibril arrays. Journal of the Mechanical Behavior of Biomedical Materials, 103563. DOI: 10.1016/j.jmbbm.2019.103563
198. Stipsitz, M., Zysset, P. K., Pahr, D. H. (2019). Efficient materially nonlinear μFE solver for simulations of trabecular bone failure. Biomechanics and Modeling in Mechanobiology, 19(5), 861-874. DOI:10.1007/s10237-019-01254-x
199. Levrero-Florencio, F., Margetts, L., Sales, E., Xie, S., Manda, K., Pankaj, P. (2016). Evaluating the macroscopic yield behaviour of trabecular bone using a nonlinear homogenisation approach. Journal of the Mechanical Behavior of Biomedical Materials, 61, 384-396. DOI: 10.1016/j.jmbbm.2016.04.008
200. Levrero-Florencio, F., Manda, K., Margetts, L., Pankaj, P. (2017). Effect of including damage at the tissue level in the nonlinear homogenisation of trabecular bone. Biomechanics and Modeling in Mechanobiology, 16(5), 1681-1695. DOI: 10.1007/s10237-017-0913-7
201. Levrero-Florencio, F., Manda, K., Margetts, L., Pankaj, P. (2017). Nonlinear homogenisation of trabecular bone: Effect of solid phase constitutive model. Proceedings of the Institution of Mechanical Engineers H: Journal of Engineering in Medicine, 231(5), 405-414. DOI: 10.1177/0954411916676220
202. Liu, C., Huang, Y., Stout, M. G. (1997). On the asymmetric yield surface of plastically orthotropic materials: A phenomenological study. Acta Materialia, 45(6), 2397-2406. DOI: 10.1016/S1359-6454(96)00349-7
203. Hou, Y., Min, J., Stoughton, T. B., Lin, J., Carsley, J. E., Carlson, B. E. (2020). A non-quadratic pressure-sensitive constitutive model under non-associated flow rule with anisotropic hardening: Modeling and validation. International Journal of Plasticity, 135, 102808. DOI: 10.1016/j.ijplas.2020.102808
204. Zolochevskii, A. A. (1986). Theory of cylindrical shells of anisotropic materials of different moduli. Soviet Applied Mechanics, 22(3), 230-235. DOI: 10.1007/BF00887243
205. Altenbach, H., Dankert, M., Zolochevsky, A. (1989). Konstitutive Gleichungen der nichtlinearen Elastizitätstheorie auf der Grundlage von 3 Invarianten des Spannungstensors. Technische Mechanik, 10(4), 211-217. https://www.researchgate.net/publication/259737689
206. Sun, J. Y., Zhu, H. Q., Qin, S. H., Yang, D. L., He, X. T. (2010). A review on the research of mechanical problems with different moduli in tension and compression. Journal of Mechanical Science and Technology, 24(9), 1845-1854. DOI: 10.1007/s12206-010-0601-3
207. Patel, B. P., Khan, K., Nath, Y. (2014). A new constitutive model for bimodular laminated structures: Application to free vibrations of conical/cylindrical panels. Composite Structures, 110, 183-191. DOI: 10.1016/j.compstruct.2013.11.008
208. Du, Z., Zhang, G., Guo, T., Tang, S., Guo, X. (2020). Tension-compression asymmetry at finite strains: A theoretical model and exact solutions. Journal of the Mechanics and Physics of Solids, 143, 104084. DOI: 10.1016/j.jmps.2020.104084
209. Latorre, M., Montáns, F. J. (2020). Bi-modulus materials consistent with a stored energy function: Theory and numerical implementation. Computers & Structures, 229, 106176. DOI: 10.1016/j.compstruc.2019.106176
210. Qiu, H., Yang, H., Tang, S., Guo, X., Huang, J. (2022). A data-driven approach for modeling tension–compression asymmetric material behavior: Numerical simulation and experiment. Computational Mechanics, 69(1), 299-313. DOI: 10.1007/s00466-021-02094-2
211. Zolochevsky, A. (2008). Degradation of perovskite-type ceramic membranes determined by defect chemistry modeling and chemically induced stress analysis. Journal of the National Technical University "Kharkiv Polytechnic Institute": Machine-building and CAD, (2), 95-104. https://www.researchgate.net/publication/270282346
212. Zolochevsky, A., Tkachuk, N. N., Viricelle, J. P., Pijolat, C. (2007). Chemically induced stresses in the cathode of single chamber solid oxide fuel cell. Journal of the National Technical University "Kharkiv Polytechnic Institute": Machine-building and CAD, (23), 148-157. https://www.researchgate.net/publication/259727171
213. Zolochevsky, A. A., Goncharova, G. V., Minko, A. I., Shalashova, I. V. (2008). Modelling of diffusion induced stresses affected by the psychoactive media in the blood vessels of biomechanical system. Journal of the National Technical University "Kharkiv Polytechnic Institute": Machine-building and CAD, (9), 90-97. https://www.researchgate.net/publication/270282537
214. Eggen, C., Lin, Y. S., Goncharova, G., Zolochevsky, A. (2009). Diffusion characteristics of a supported lipid

bilayer membrane on a dense cylindrical silica optical fibrous support. In 2009 AIChE Annual Meeting, Nashville, USA, 20p. https://www.researchgate.net/publication/267317075
215. Zolochevsky, A., Grabovskiy, A. V., Parkhomenko, L., Lin, Y. S. (2012). Coupling effects of oxygen surface exchange kinetics and membrane thickness on chemically induced stresses in perovskite-type membranes. Solid State Ionics, 212, 55-65. DOI: 10.1016/j.ssi.2012.02.003
216. Zolochevsky, A., Parkhomenko, L., Kühhorn, A. (2012). Analysis of oxygen exchange-limited transport and chemical stresses in perovskite-type hollow fibers. Materials Chemistry and Physics, 135(2-3), 594-603. DOI: 10.1016/j.matchemphys.2012.05.031
217. Zolochevsky, A., Grabovskiy, A.V., Parkhomenko, L., Lin, Y. S. (2013). Transient analysis of oxygen non-stoichiometry and chemically induced stresses in perovskite-type ceramic membranes for oxygen separation. Journal of the National Technical University "Kharkiv Polytechnic Institute": Machine-building and CAD, (1), 179-189. https://www.researchgate.net/publication/270280587
218. Mahnken, R., Stein, E. (1997). Parameter identification for finite deformation elasto-plasticity in principal directions. Computer Methods in Applied Mechanics and Engineering, 147(1-2), 17-39. DOI: 10.1016/S0045-7825(97)00008-X
219. Mahnken, R. (2017). Identification of material parameters for constitutive equations. In Stein E., de Borst R., Hughes, T.J.R. (eds.), Encyclopedia of Computational Mechanics (pp. 1-21), Volume 4. Weinheim: Wiley, Second Edition. DOI: 10.1002/9781119176817.ecm2043
220. Mahnken, R. (2022). Strain mode-dependent weighting functions in hyperelasticity accounting for verification, validation, and stability of material parameters. Archive of Applied Mechanics, 92(3), 713-754. DOI: 10.1007/s00419-021-02069-y
221. Zolochevsky, A., Sklepus, S., Kozmin, Y., Kozmin, A., Zolochevsky, D., Betten, J. (2004). Constitutive equations of creep under changing multiaxial stresses for materials with different behavior in tension and compression. Forschung im Ingenieurwesen, 68(4), 182-196. DOI: 10.1007/s10010-003-0123-6
222. Zolochevsky, A., Voyiadjis, G. Z. (2005). Theory of creep deformation with kinematic hardening for materials with different properties in tension and compression. International Journal of Plasticity, 21(3), 435-462. DOI: 10.1016/j.ijplas.2003.12.007
223. Altenbach, H., Zolochevsky, A. (1994). A unified model of low cycle fatigue damage. In Fourth International Conference on Biaxial/Multiaxial Fatigue, (pp. 117-128), Volume 2. Paris: Societe Francaise de Metallurgie de Materiaux. https://www.researchgate.net/publication/264708215
224. Altenbach, H., Zolochevsky, A. (1996). A generalized fatigue limit criterion and a unified theory of low-cycle fatigue damage. Fatigue & Fracture of Engineering Materials & Structures, 19(10), 1207-1219. DOI: 10.1111/j.1460-2695.1996.tb00944.x
225. Zolochevsky, A., Obataya, Y. (2000). A microcrack description of unilateral fatigue damage in crystalline solids. Memoirs of the Faculty of Engineering, Fukui University, 48(2), 303-312. https://www.researchgate.net/publication/259726020
226. Zolochevsky, A., Obataya, Y., Betten, J. (2000). Critical plane approach with two families of microcracks for modelling of unilateral fatigue damage. Forschung im Ingenieurwesen, 66(2), 49-56. DOI: 10.1007/s100100000036
227. Zolochevsky, A., Itoh, T., Obataya, Y., Betten, J. (2000). A continuum damage mechanics model with the strain-based approach to biaxial low cycle fatigue failure. Forschung im Ingenieurwesen, 66(2), 67-73. DOI: 10.1007/s100100000040
228. Zolochevsky, A., Stepchenko, A., Betten, J. (2001). A microcrack description of multiaxial low cycle fatigue. Technische Mechanik, 21(2), 109-120. https://www.researchgate.net/publication/259910768
229. Zolochevsky, A., Obataya, Y., Itoh, T. (2001). A combined critical plane and strain-based approach with two families of microcracks to multiaxial low cycle fatigue damage. Journal of Theoretical and Applied Mechanics, 31(2), 65-77. https://www.researchgate.net/publication/264708215
230. Susmel, L. (2011). On the overall accuracy of the modified Wöhler curve method in estimating high-cycle multiaxial fatigue strength. Frattura Ed Integrità Strutturale, 5(16), 5-17. DOI: 10.3221/IGF-ESIS.16.01
231. Zhan, Z., Li, H., Lam, K. Y. (2019). Development of a novel fatigue damage model with AM effects for life prediction of commonly-used alloys in aerospace. International Journal of Mechanical Sciences, 155, 110-124. DOI: 10.1016/j.ijmecsci.2019.02.032
232. Sun, W., Sun, Z., Lu, Q., Chen, X., Song, Y. (2019). Fatigue hysteresis loops simulation of SiCf/Ti composites under two-stage cyclic loading. Applied Composite Materials, 26(3), 1041-1057. DOI: 10.1007/s10443-019-09765-7
233. Liu, B., Yan, X. (2020). A multi-axial fatigue limit prediction equation for metallic materials. Transactions of the ASME. Journal of Pressure Vessel Technology, 142(3), 034501. DOI: 10.1115/1.4046217
234. Papuga, J., Cízová, E., Karolczuk, A. (2021). Validating the methods to process the stress path in multiaxial high-cycle fatigue criteria. Materials, 14(1), 206. DOI: 10.3390/ma14010206
235. Scherer, J. M., Besson, J. (2022). Implementation of constitutive equations for single crystals in finite

element codes. In Cailletaud G., Cormier J., Eggeler G., Maurel V., Naze L. Nickel Base Single Crystals Across Length Scales (pp. 473-494). Amsterdam: Elsevier. DOI: 10.1016/B978-0-12-819357-0.00027-5

236. Sattar, M., Othman, A. R., Kamaruddin, S., Akhtar, M., Khan, R. (2022). Limitations on the computational analysis of creep failure models: A review. Engineering Failure Analysis, 134(1), 105968. DOI: 10.1016/j.engfailanal.2021.105968
237. Zolochevsky, A., Becker, A. A. (2011). Introduction to ABAQUS. Kharkiv: Business Investor Group. https://www.researchgate.net/publication/335652019
238. Zolochevsky, A., Sklepus, S., Hyde, T. H., Becker, A. A., Peravali, S. (2009). Numerical modeling of creep and creep damage in thin plates of arbitrary shape from materials with different behavior in tension and compression under plane stress conditions. International Journal for Numerical Methods in Engineering, 80(11), 1406-1436. DOI: 10.1002/nme.2663
239. Zolochevsky, A., Sklepus, S., Galishin, A., Kühhorn, A., Kober, M. (2014). A comparison between the 3D and the Kirchhoff-Love solutions for cylinders under creep-damage conditions. Technische Mechanik, 34(2), 104-113. https://www.researchgate.net/publication/262198221
240. Sklepus, S. N., Zolochevskii, A. A. (2014). A study of the creep damageability of tubular solid oxide fuel cell. Strength of Materials, 46(1), 49-56. DOI: 10.1007/s11223-014-9514-1
241. Galishin, A. Z., Zolochevsky, A. A., Sklepus, S. M. (2018). Study of creep and damage for a hollow cylinder on the basis of space and refined shell models. Journal of Mathematical Sciences, 231(5), 629-640. DOI: 10.1007/s10958-018-3840-y
242. Zolochevsky, A., Galishin, A., Sklepus, S., Parkhomenko, L., Gnitko, V., Kühhorn, A., Leyens, C. (2013). Benchmark creep tests for thermal barrier coatings. Journal of the National Technical University "Kharkiv Polytechnic Institute": Machine-building and CAD, (23), 158-178. https://www.researchgate.net/publication/270281555
243. Zolochevsky, A., Parkhomenko, L., Gnitko, V., Kühhorn, A., Kober, M. (2014). Damage accumulation in multilayer thin films on gamma titanium aluminides. Journal of the National Technical University "Kharkiv Polytechnic Institute": Machine-building and CAD, (29), 182-195. https://www.researchgate.net/publication/270281921
244. Zolochevsky, A. (2015). Damage development in thermal and environmental barrier coating systems for aerospace applications. Technical Report, Kharkiv: Research Center «Polytech», 26p. https://www.researchgate.net/publication/342493554
245. https://en.wikipedia.org/wiki/Battle_of_Kharkiv_(2022)